Available online at www.sciencedirect.com
ScienceDirect
Solar Energy 85 (2011) 1264–1282
SOLAR ENERGY
www.elsevier.com/locate/solener

Colloidal quantum dot solar cells

Saim Emin *, Surya P. Singh [1], Liyuan Han *, Norifusa Satoh [1], Ashraful Islam [1]

National Institute for Materials Science (NIMS), Advanced Photovoltaics Center, Sengen 1-2-1, Tsukuba 305-0047, Japan

Available online 12 March 2011

Communicated by: Associate Editor Frank Nuesch

Abstract

In recent years colloidal quantum dots solar cells have been the subject of extensive research. A promising alternative to existing silicon solar cells, quantum dot solar cells are among the candidates for next generation photovoltaic devices. Colloidal quantum dots are attractive in photovoltaics research due to their solution processability which is useful for their integration into various solar cells. Here, we review the recent progresses in various quantum dot solar cells which are prepared from colloidal quantum dots. We discuss the preparation methods, working concepts, advantages and disadvantages of different device architectures. Major topics discussed in this review include integration of colloidal quantum dots in: Schottky solar cells, depleted heterojunction solar cells, extremely thin absorber solar cells, hybrid organic–inorganic solar cells, bulk heterojunction solar cells and quantum dot sensitized solar cells. The review is organized according to the working principle and the architecture of photovoltaic devices.

Keywords: Colloidal quantum dot; Solar cell; Sensitizer

1. Introduction

Increasing worldwide demand for energy and limited fossil fuels reserves on the planet require development of reliable and renewable energy sources. Among the various technologies available nowadays, photovoltaics is believed to be one of the cleanest ways in achieving this goals. However, efforts are still needed to make photovoltaics cost competitive over other established technologies for energy production (Service, 1996). Integration of nanostructured materials in photovoltaic devices has been demonstrated to open the possibilities to develop low-cost solar cells (Chiba et al., 2006). In recent years, inorganic semiconductor nanocrystals (also known as Quantum Dots, QDs) have been found to be promising for next generation solar cell (Robel et al., 2006; Kamat, 2007). QDs have been explored due to their size and compositional dependent absorption (Peng et al., 2000; Vomeyer et al., 1994; Emin et al., 2009a,b, 2010; Yu et al., 2003). Previously unachievable with bulk semiconductors, the QDs allow energy level matching between desired donor and acceptor materials which is crucial in designing efficient photovoltaic devices. Moreover, QDs can be solution processed and could be an alternative to commonly employed sensitizer molecules (Bang and Kamat, 2009). During the last decade colloidal QDs have been integrated in different types of solar cells such as: Schottky solar cells (Johnston et al., 2008; Koleilat et al., 2008), depleated heterojunction solar cells (Pattantyus-Abraham et al., 2010), extremely thin absorber cells (Ernst et al., 2003), hybrid polymer solar cells (Günes et al., 2007a,b; Yun et al., 2009), inorganic–organic heterojuction solar cells (Chang et al., 2010; Leschkies et al., 2007) and quantum dot sensitized solar cells (QDSSCs) (Lee et al., 2008a; Kongkanand et al., 2008). Fig. 1 shows the typical device architectures used in QDs solar cells. The great interest in QDs solar cells also arises from the phenomenon called multiexciton generation (MEG) that can be used in achieving high efficiency solar cells. Quantum

* Corresponding authors. Tel.: +81 29 859 2305; fax: +81 29 859 2386.
E-mail address: EMIN.Saim@nims.go.jp (S. Emin, L. Han).
[1] Tel.: +81 29 859 2305; fax: +81 29 859 2386.

0038-092X/$ - see front matter © 2011 Elsevier Ltd. All rights reserved.
doi:10.1016/j.solener.2011.02.005

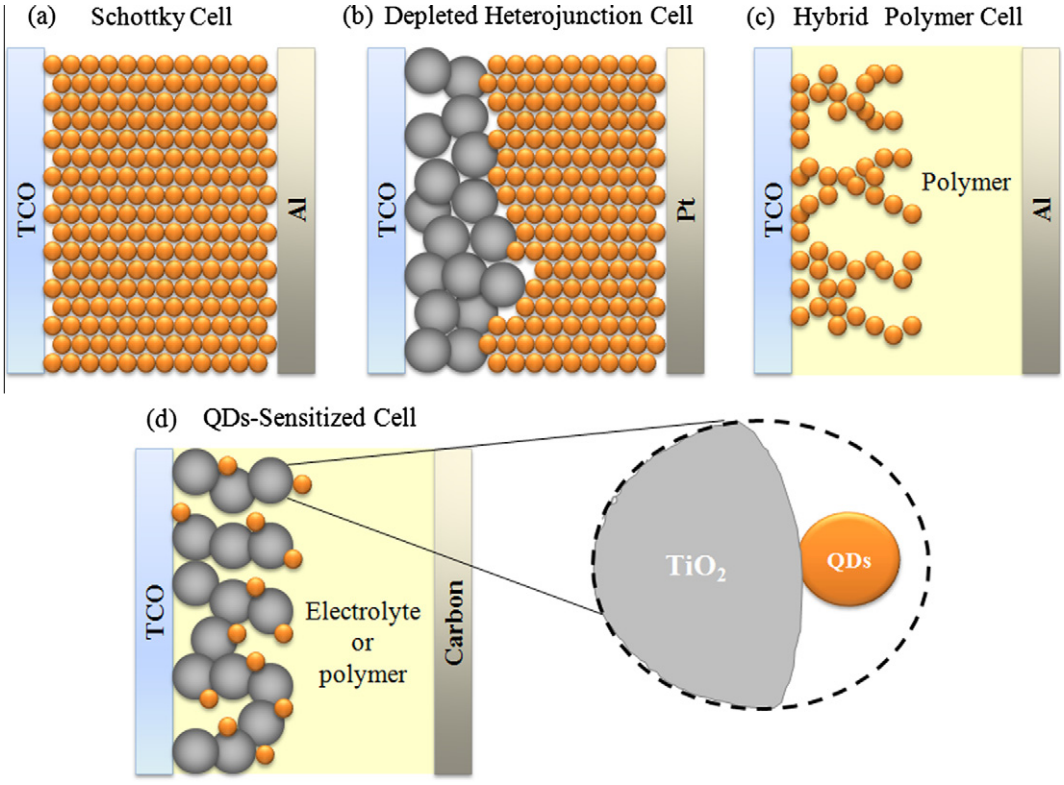

Fig. 1. Comparison of various QDs based photovoltaics cells. (a) Schottky cell; (b) depleted heterojunction cell; (c) hybrid polymer solar cells and d) QDs sensitized solar cell.

dot solar cells offer the possibility of boosting the energy conversion efficiency beyond the traditional Schockley and Queisser limit of 32% for Si based solar cells (Shockley and Queisser, 1961). In recent years, efficient MEG processes have been reported in PbS (Sukhovatkin et al., 2009), PbSe (Pijpers et al., 2009), PbTe (Murphy et al., 2006), CdSe (Schaller et al., 2006) and Si QDs (Beard et al., 2007). However, realization of this process in solar cells has not been achieved yet. Toward realization of this goal fundamental studies are needed to be carried out such as ultrafast exciton dynamic studies as well as better device architecture.

In recent years, several review articles have appeared on quantum dot solar cells such as bulk heterojunction and QDSSCs. Since most of the research efforts have been concentrated on QDSSCs several review have appeared on this topic concerning different aspects of QDSSCs. One of the first reviews on QDSSCs had been written by Kamat (2008). In the same year Hodes (2008) gave comparison of the working principles of QDSSCs and dye sensitized solar cells. Similarly, a review article on QDSSCs has been written by Rühle et al. (2010) emphasizing the role of molecular dipoles in energy-level alignment of QDs. Colloidal quantum dots have been used in bulk heterojunction solar cells as well. Arici and Sariciftci (2004) and Kumar and Scholes (2008) have reviewed the recent progresses in this field. Due to the great research interests in one-dimensional (1D) structures Yun et al. (2009) highlighted integration of colloidal nanoparticles in nanorods and nanowires based solar cells. In addition, Talapin et al. (2010) has reviewed a wide range of applications of quantum dots in optoelectronic devices such as photodetectors, light emitting diodes and briefly about quantum dot solar cells.

Although review articles on this topic exist there is no systematic review which describes the working principles of various types of quantum dot solar cells. Motivated by the fascinating rapid growth in this field during the last couple of years, we review the recent advances in colloidal quantum dot solar cells. Here we discuss the processing conditions of colloidal quantum dots and fabrication steps of photovoltaic devices. We explore the different types of QDs solar cells in one review material allowing the reader to easily compare the advantages and disadvantages of each device structure. In addition, we discuss the working principles of the given quantum dot solar cells.

2. Basic terms for photovoltaic performance

The performance of a solar cell can be estimated from its current–voltage diagram. Due to the differences in operation mechanism of the solar cell here we will only introduce basic notations regarding the current–voltage diagrams.

Air mass 1.5 (AM 1.5): A standard terrestrial solar spectral irradiance distribution.

Short-circuit current (J_{SC}): The current that flows in a photovoltaic device when illuminated and its electrodes are connected.

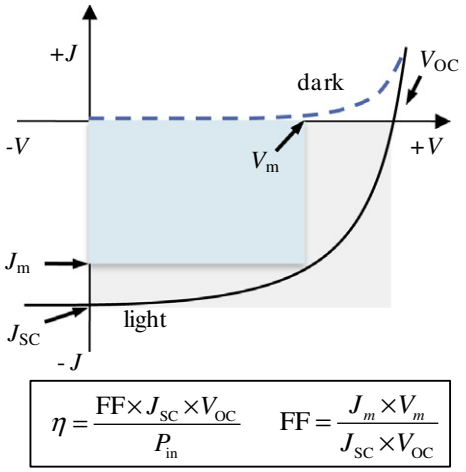

Fig. 2. Current–voltage characteristics of a solar cell under dark and under illumination. The efficiency (η) of a solar cell is defined as the ratio of input power (P_{in}) and output power (P_{out}). J_m and V_m are the current and voltage at the maximum power point.

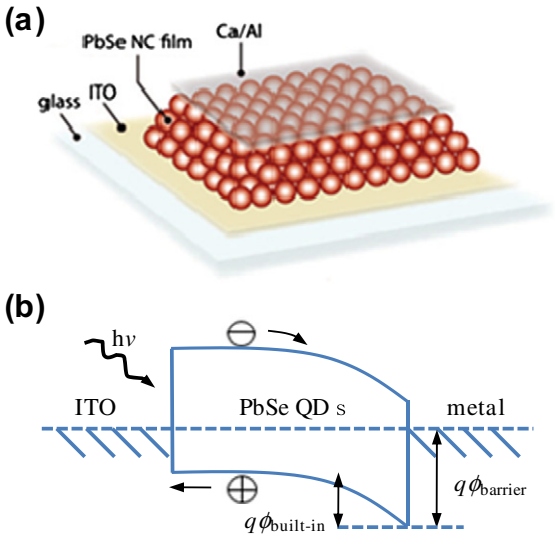

Fig. 3. (a) Scheme of a Schottky device and (b) its equilibrium band diagram. Band bending occurs at the interface between the QDs and evaporated negative electrode. The data are taken with permission from Law et al. (2008).

Open-circuit voltage (V_{OC}): The voltage provided by an illuminated photovoltaic device when no external load is connected.

Fill factor (FF): The ratio of the actual power a solar cell can supply to the maximum predicted by the product of its short-circuit current and its open-circuit voltage.

Power conversion efficiency (η): The power conversion efficiency of a device is defined as the ratio between the maximum electrical power generated and the incident optical power (P_{in}).

Fig. 2 shows current–voltage characteristics of a solar cell. In the dark, the current–voltage curve is strongly asymmetric and shows a diode behavior. Under illumination, the current–voltage curve exhibit a vertical shift caused by light-induced current generation. More details regarding the operation principles of solar cells are given in review articles and textbooks (Sun and Sariciftci, 2005; Günes et al., 2007a,b; Thompson and Fréchet, 2008).

3. Schottky solar cells

A Schottky junction solar cell is likely the simplest photovoltaic device that can be fabricated. Colloidal quantum dot sensitized solar cells using simple Schottky junction offer potentials where solution-processed QDs can be applied to achieve low-cost solar devices (Law et al., 2008). Schottky types of solar cells are attractive due to several reasons: Firstly, they can be prepared by spray-coating or inkjet printing from solution phase. Secondly, thin layer (~100 nm) of absorber QDs is required in the photovoltaic cell. Fig. 3 shows a typical device structure of Schottky cell. The cell is described with band bending at the interface of a metal and a p-type semiconductor. This band bending makes a depletion region due to a charge transfer from the electron-accepting contact to the p-type QDs film. The resultant Schottky barrier favors the extraction of electrons from the device while presenting a barrier for hole withdrawal (Clifford et al., 2007). From the perspective of charge-carrier transport, drift and diffusion play an important role in the operation of these devices. Achieving high efficiency in these cells requires carrier's extraction before they recombine. This requires that the mobility, , of each carrier exceed $\phi_{built\text{-}in}/d^2$, where the $\phi_{built\text{-}in}$ is the built-in potential, τ is the carrier lifetime, and d is the device thickness (Klem et al., 2007). The measurement of mobility has yielded at best 2×10^{-3} cm^2/Vs making the QDs Schottky devices attractive. The barrier height of the built-in potential can be estimated from the relation: $q\phi_{built\text{-}in} = E_g - q(\phi_m - \chi)$, where E_g is the bandgap of the semiconductor QDs, q is the charge of an electron, ϕ_m is the work function of the metal and χ the electron affinity of the semiconductor. So far, the Schottky devices have shown certain disadvantages as well. First, many minority carriers (here electrons) must travel the entire film before reaching their destination electrode and are therefore more liable for recombination. Second, in the Schottky device, the open-circuit voltage is often limited by Fermi-level pinning due to defect states at the metal–semiconductor interface. Such effects are important in photovoltaics as they limit the open-circuit voltage that a device can provide.

Most of the studies on Schottky solar cells are based on near-infrared (NIR) wavelength absorbing nanomaterials such as Si (Liu and Kortshagen, 2010), CdTe (Olson et al., 2010), PbS (Tang et al., 2010; Klem et al., 2008) and PbSe (Luther et al., 2008). The extensive research on lead chalcogenides is due to their large exciton Bohr radii (PbS 18 nm and PbSe 47 nm). The larger Bohr radius delocalizes the carriers, establishing greater electronic coupling between nanocrystals, which can diminish the effect of

nanocrystal surface traps and therefore facilitate charge transport. Fig. 4 shows typical current–voltage and capacitance–voltage curves from a Schottky cell composed of CdTe nanorods (Olson et al., 2010). The device used in the study produces a power conversion efficiency of 5.3%, a short circuit–current (J_{SC}) of 21.6 mA/cm^2, an open-circuit-voltage (V_{OC}) of 540 mV and a fill-factor of 45.5%. This is among the highest efficiency reported for this type of device. As shown in Fig. 4b, capacitance-volatge measurements (in dark) suggest that this device exhibit a Schottky barrier. From the Mott-Schottky analysis it can be estimated the built-in potential, depletion width, and carrier concentration. The capacitance of the depletion region which is used to calculate the acceptor density and built in potential is given as (Olson et al., 2010):

$$\frac{1}{C^2} = \frac{2}{A^2 e \varepsilon_0 \varepsilon N_a}\left(\phi_{built\text{-}in} - \frac{k_B T}{e} - V\right) \quad (1)$$

where A is the device area, V is the applied bias, N_a is the acceptor density, ε_o is the permittivity of vacuum and ε are the static permittivity of the semiconductor. From the fit of Eq. (1) as shown in Fig. 4b the carrier concentration is calculated to be 7×10^{16} cm^{-3}.

One of the actively studied materials in Schottky solar cells is PbS. Most of the contributions in this type of device architecture are achieved by Nozik's and Sargent's groups. By using PbS QDs the power conversion efficiencies of Schottky devices have been increased up to 3.6% (100 mW/cm^2, AM1.5) (Debnath et al., 2010). Moreover, these devices give lower efficiencies than those with CdTe QDs, which could be attributed to the shape of used nanocrystals. With expectation to improve the efficiencies of Schottky solar cells ternary PbS_xSe_{1-x} QDs have been used as well (Ma et al., 2009). As an example is $PbS_{0.7}Se_{0.3}$ QDs Schottky device that exhibit a power conversion efficiency of 3.3% with a $J_{SC} = 14.8$ mA/cm^2, a $V_{OC} = 0.45$ V, and a FF = 50% (100 mW/cm^2). Needless to be mentioned that PbS and PbSe QDs devices prepared under similar conditions yield 2-fold lower efficiencies. In addition, the differences in power conversion efficiencies obtained by different groups could be attributed to film processing condition and the quality of used nanocrystals.

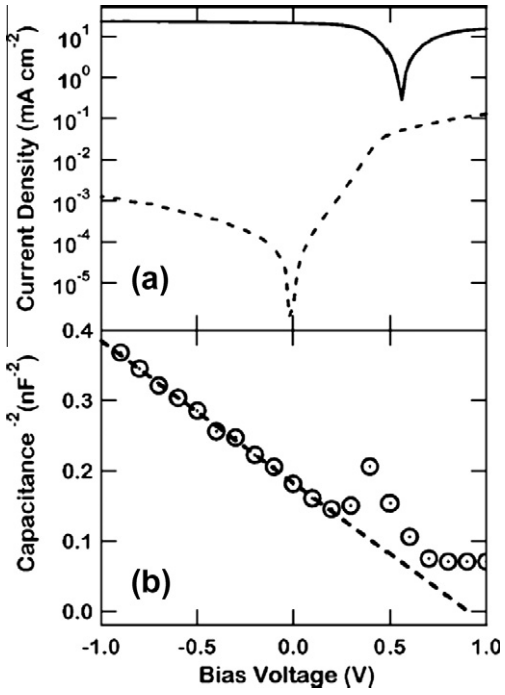

Fig. 4. (a) Current–voltage and (b) capacitance–voltage curves of CdTe Schottky devices. Measurements in (a) are conducted at 1 sun illumination (solid) and in dark (dash). Measurements in (b) are taken at 50 Hz. Data are taken with permission from Olson et al. (2010).

4. Depleted heterojunction solar cells

Most of the researches on depleted heterojunction solar cells are concentrated on lead chalcogenide quantum dots. By using PbS QDs in depleted-heterojunction device architecture the power conversion efficiency of quantum dot solar cells were boosted up to 5.1% (100 mW/cm^2, AM 1.5) (Pattantyus-Abraham et al., 2010). These devices overcome the limitations of the Schottky type cells associated with the low built-in voltages. Fig. 5 shows a typical scheme of a depleted-heterojunction device. The photovoltaic cell architecture in general consists of a QDs layer sandwiched between an electron transporting layer (usually TiO_2) and a metal electrode (Fig. 5). In such kind of structure, electrons flow toward the TiO_2 layer rather than the evaporated metal contact, thus creating an inverted polarity (Debnath et al., 2010). Moreover, hole transfer from TiO_2 to QDs is prohibited which allows efficient carrier separation. Depleted heterojunction cells overcome the

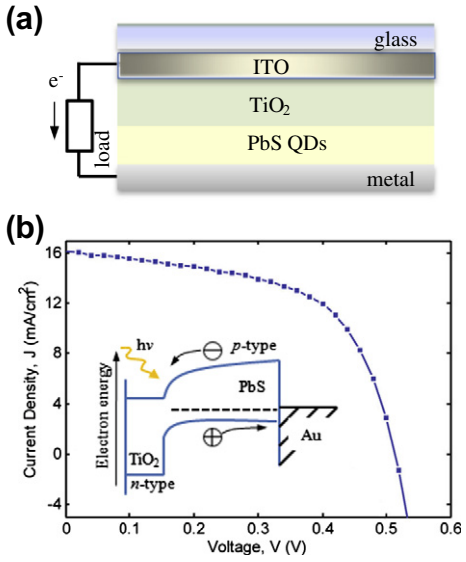

Fig. 5. (a) Scheme of depleted-heterojunction device. (b) Current–voltage curve from FTO/TiO_2/PbS QD/Au photovoltaic device. The inset in (b) shows band diagram of the photovoltaic cell. Reprinted with permission from Pattantyus-Abraham et al. (2010).

limitations of Schottky solar cells in several ways. First, the depleted heterojunction design benefits from minority carrier separation due to the placement of the junction on the illumination side. Second, back electron transfer from TiO_2 to QDs is suppressed by the built-in field of the depletion region. Third, devices show improved open-circuit voltages due to better carrier separation at the QDs/TiO_2 interface.

From energy diagram perspectives nanocrystalline PbS is an ideal light harvesting material in the near-infrared region since it can be used as electron donor for wide band-gap materials (TiO_2 or ZnO) in heterojunction solar cells (Hyun et al., 2008). Luther et al. (2010) demonstrated that *p*-type PbS QDs in contact with *n*-type ZnO nanoparticles form a *p*-*n* heterojunction. Using these material they fabricated a solar device that gave certified power conversion efficiency of 2.9%, $J_{SC} = 8.9\ mA/cm^2$ and $V_{OC} = 0.59\ V$ (100 mW/cm^2, AM 1.5). Moreover, this efficiency is obtained from a device with an aperture area of 0.029 cm^2. Similarly, Ju et al. (2010) used TiO_2 nanoparticles instead of ZnO in order to prepare PbS/TiO_2 heterojunction devices. They studied the effect of temperature on the power conversion efficiency of photovoltaic cells. They recorded a power conversion efficiency of about 3% (100 mW/cm^2), a $J_{SC} = 28.6\ mA/cm^2$, a $V_{OC} = 0.66\ V$, and a FF = 42.6% which is achieved at 170 K. The remarkable efficiency is due to an increase in charge transport across the PbS QDs layer at low-temperatures. Furthermore, depleted hetrojunction solar cells have been studied by Norris group as well (Leschkies et al., 2009). As an example the device is composed of an ITO electrode, a *n*-type ZnO nanoparticles, a PbS QDs layer and a thin electron blocking layer of N,N′-bis(1-naphthalenyl)-N,N′bis(phenylbenzidine). To achieve built-in potential on top of the electron blocking layer is deposited an element gold (Fig. 6a). Typical photovoltaic cell demonstrated a $J_{SC} = 15.7\ mA/cm^2$, a $V_{OC} = 0.39\ V$ and a $\eta = 1.6\%$ (100 mW/cm^2, AM1.5). An important difference between the device structure given above and the traditional *p*–*n* heteorojunction is that the band-gap of *p*-type QDs can be varied in the case of depleted heterojunction solar cells. Furthermore, Norris group observed a linear change in V_{OC} by increasing QDs sizes in those devices (Fig. 6b). The latter is explained with the ambipolar nature of QDs. Since, PbS QDs are not entirely p-type it causes shift in the Fermi level which brings deviation from the characteristic of an ideal *p*–*n* heterojunction. Furthermore, they conclude that these devices operate more like excitonic solar cells. Similarly, decrease in V_{OC} versus nanocrystal size is observed for PbS depleted heterojunction solar cells by Sargent group as well (Pattantyus-Abraham et al., 2010). Regardless of the operational principles these devices constitute a novel class of heterojunction solar cells.

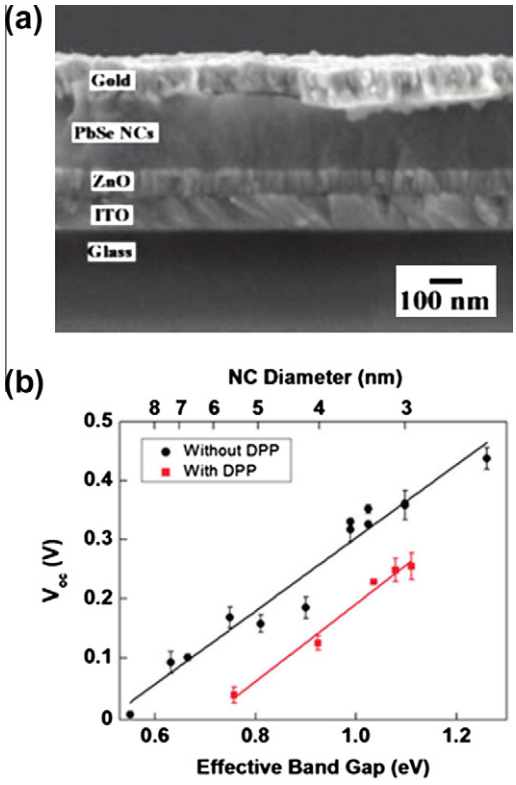

Fig. 6. (a) Cross-sectional scanning electron micrograph of ITO/PbSe QDs/ZnO/Au heterojunction device. (b) Dependence of V_{OC} on the diameter and effective band-gap of PbS QDs. Nanocrystals are synthesized in the presence and absence of diphenylphosphine (DPP). Reprinted with permission from Leschkies et al. (2009).

5. Extremely thin absorber (ETA) solar cells

Extremely thin absorber (ETA) solar cells have been extensively studied during the past two decades (Könenkamp, 2008). Here we provide only a brief overview of this type of device architecture focusing on quantum dots. Based on the deposition method of the absorber layer there is a large variety of approaches for preparing ETA solar cells. The most common approaches are successive ion-layer adsorption and reaction (SILAR), ion layer gas reaction (ILGAR), electrodeposition, atomic layer deposition (ALD) and finally plasma-assisted chemical vapor deposition. Fig. 7 shows a typical schematic diagram of ETA solar cell with porous geometry. The cell consists of a thin intrinsic (*i*-type) layer embedded between two transport (*n*-type and *p*-type) layers. The transport layers serve for the purpose of transferring the photogenerated carriers from the absorber layer toward the contacts. Historically inorganic hole transporting copper compounds such as CuI, CuSCN and $CuAlO_2$ were often employed in ETA solar cells (Levy-Clément et al., 2005; Kawazoe et al., 1997). An example of this kind of device is ZnO/CdSe/CuSCN architecture, based on *n*-type ZnO nanowires and *p*-type CuSCN hole transporting material (Ernst et al., 2003). In terms of their energy band-gap, the two transparent *p*- and *n*-type semiconductors develop a high electrical field at their interface. Meanwhile, the thickness of CdSe layer greatly affects the kinetics of photogenearted electrons at the ZnO interface. A fabricated device showed a $J_{SC} = 4\ mA/cm^2$, a $V_{OC} = 0.5\ V$ and an overall power

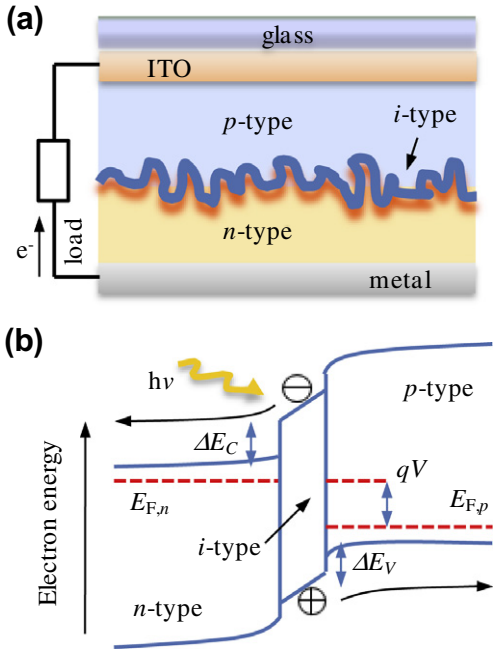

Fig. 7. (a) Scheme of an ETA solar cells. (b) Band structure of the ETA cell showing quasi Fermi levels $E_{F,n}$ and $E_{F,p}$ in the electron and hole conductor. The difference between these two levels determines the photovoltage V. The conduction-band and valence-band offsets E_C and E_V between the electron and hole conductors should be in the order of ~0.2–0.3 V.

conversion efficiency of 2.3% (36 mW/cm^2). Besides nanowires, mesoporous TiO_2 substrate may also be considered as an ideal matrix material for quantum dots. For this purpose ETA soar cells made of thin absorber layer of Sb_2S_3 QDs on mesoporous TiO_2 with hole conducting CuSCN layer have been studied as well (Itzhaik et al., 2009). Similar to CdSe, the Sb_2S_3 with a band-gap at about 1.7 eV is an ideal light harvesting material in the visible region of electromagnetic spectrum. Under 1 sun illumination a typical device demonstrated a $J_{SC} = 14.1$ mA/cm^2, a $V_{OC} = 0.49$ V, a FF = 48.8% and a conversion efficiency of 3.3%. Moreover, this device exhibited good stability in air for several days. This was attributed to the formation of surface Sb_2O_3 layer on top of Sb_2S_3 QDs when the device was exposed to air. The surface oxides presumably act as a passivation layer which reduces the recombination events between in Sb_2S_3 QDs. Although some experimental efforts have been done in this area the power conversion efficiencies of ETA cells have so far remained well below 4% (Wienke et al., 2003). Modelling calculations indicate that 15% efficient CdTe ETA cells can be prepared (Taretto and Rau, 2005). If efficiency improvement of this order can be achieved, ETA could provide a cheaper alternative to existing solar cells.

6. Inorganic–organic heterojunction solar cells

Inorganic–organic heterojunction devices with sensitizer nanocrystals are among the possible structures which can be applied in large scale production (Chang et al., 2010). The working concept of these devices has common points with ETA solar cells. However, due to the linking mode between QDs and semiconductor oxides here we divide them into a separate class called inorganic–organic heterojunction cells. Incorporation of organic hole transporting materials in these devices is found to give better performances compared with ETA solar cells where they are used as solid state hole semiconductors. In this class of devices Sb_2S_3 QDs have exhibited the highest reported efficiency, where Chang et al. (2010) achieved 5.13% photoconversion efficiency (100 mW/cm^2, AM1.5) by using sensitizer Sb_2S_3 QDs and hole transporting P3HT polymer in the following cell configuration TiO_2/Sb_2S_3/P3HT/Au. Crystalline Sb_2S_3 is one of the promising semiconductor materials for photovoltaic applications because of its optimum band-gap (~1.7 eV) (Versavel and Haber, 2007). The Sb_2S_3 inorganic–organic devices perform remarkably well giving a high incident-photon-to-current efficiency (IPCE) of about 80% at its maximum value at 450 nm. Fig. 8 shows illustration of the cell configuration used in the study, absorbance spectra, IPCE spectra and current voltage spectra. This unique example demonstrates the applicability of hole transporting materials in quantum dot inorgainic–organic heterojunction devices. Although hole transporting polymers gave low conversion efficiencies in the order of 2.6% (Mozer et al., 2006) in quasi-solid-state DSSCs, it was possible to obtain promising results in quantum dot based inorganic–organic heterojunction cells. This could be explained with complete pore (TiO_2) filling of the polymer in the case of quantum dot heterojunction devices. It seems that hole transporting polymers effectively permeates the pores of QDs sensitized TiO_2 electrodes. Furthermore, by changing the morphology of metal oxides it could be possible to find an optimum pore size that could open a new door for achieving efficient hole transport across the polymers. Recent studies showed that nanowires of metal oxides present a new morphology for inorganic–organic devices. These structures are designed to achieve efficient electron transfer through the nanowires and also provide relatively large voids for the hole conducting polymer. Based on this approach Nadarajah et al. (2008) used *n*-type ZnO nanowires to fabricate inorganic–organic photovoltaic devices composed of CdSe QDs and hole transporting polymer poly[2-methoxy-5-(2′-ethyl-hexyloxy)-1,4-phenylene vinylene]) (MEHPPV). Despite expected high photocurrent efficiencies these devices showed relatively low conversion efficiencies in the order of 1% (85 mW/cm^2). This could be due to an insufficient contact between CdSe QDs and ZnO nanowires (or polymer) which may affect the electron–hole recombination dynamics. In another study inorganic–organic heterojunction devices have been fabricated by using CdSe QDs and TiO_2 nanoparticles followed the layer-by-layer protocol (Kniprath et al., 2009). As a hole transporting material poly(9,9-dioctyl-fluorene-co-N-(4-butylphenyl)diphenylamine (TFB) is used. However due to the poor interconnection between

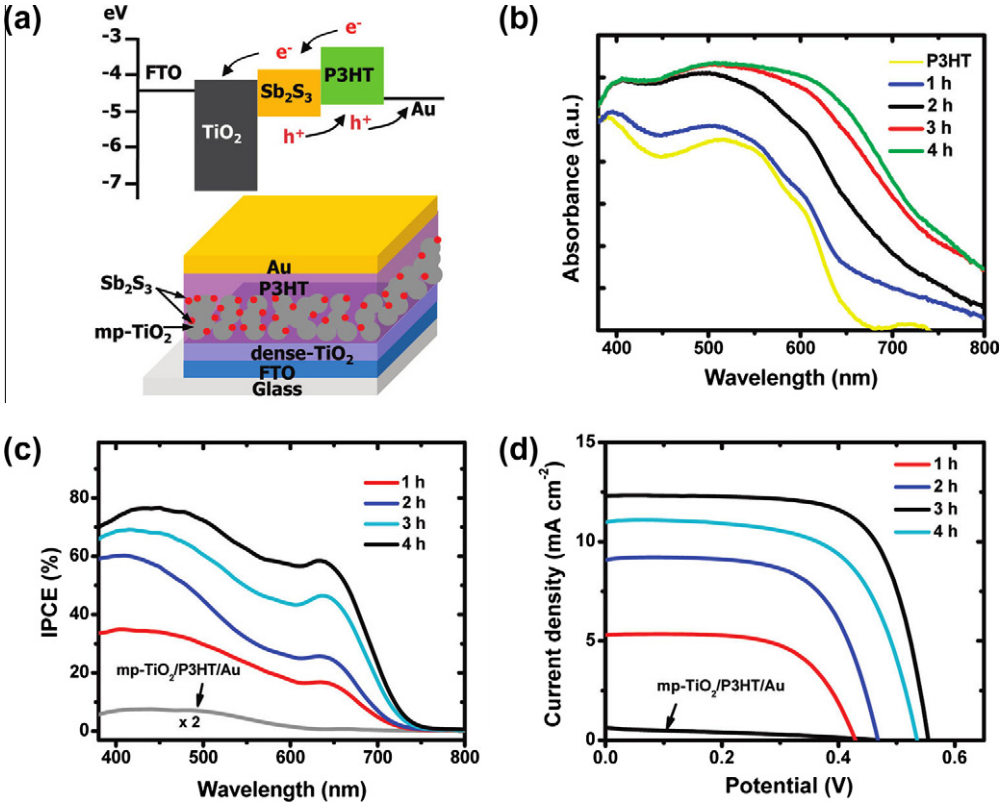

Fig. 8. (a) Energy diagram and schematic configuration of ionorganic-organic device. (b) Absorption spectra of P3HT and Sb_2S_3 deposited for various deposition times on TiO_2 electrodes. (c) IPCE spectra of TiO_2/P3HT/Au and TiO_2/Sb_2S_3/Au photovoltaic devices. (d) Current–voltage curves for devices in (c). Reprinted with permission from Chang et al. (2010).

CdSe nanoparticles and TiO_2 (or polymer) relatively low external quantum efficiencies are obtained. Typical values of photocurrents and photovoltages after sintering of the films at 250 °C are $J_{SC} = 0.05$ mA/cm^2, $V_{OC} = 1.0$ V and FF = 31% (100 mW/cm^2).

During the last decade many expectations were given to near-infrared wavelength absorbing QDs. Not long ago Plass et al. (2002) demonstrated one of the first studies on PbS QDs based inorganic–organic devices. By using a hole conducting polymer spiro-OMeTAD in the photovoltaic devices they achieved power conversion efficiencies in the order of 0.5% (10 mW/cm^2, AM1.5). The low power conversion efficiencies were explained with inefficient charge separation at the PbS/TiO_2 interface. To address the physics of charge separated states Leventis et al. (2010) examined the mechanism of charge injection and recombination at PbS/metal oxide surfaces. They found that yield of charge injection from PbS QDs to TiO_2 is relatively low compared with charge injection from PbS QDs to SnO_2 electrodes. The latter is explained with the conduction-band edge position of SnO_2 which favors electron injection from PbS QDs. Consequently the efficient electron injection from PbS to SnO_2 favors the formation of longer lived oxidized state of PbS as shown in the transient absorption spectrum of PbS QDs (Fig. 9). Furthermore, efficient electron injection from PbS QDs to TiO_2 could

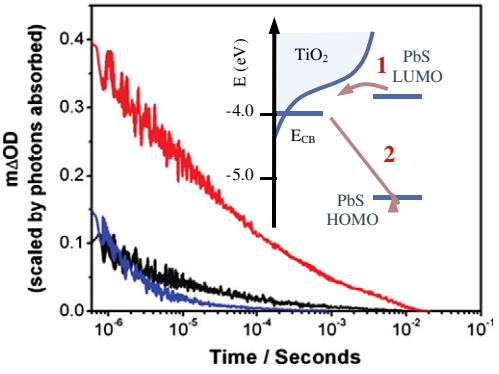

Fig. 9. Transient kinetics of PbS-localized holes (at 1600 nm) obtained from metal oxide/PbS QD electrodes. Data are obtained using mesoporous TiO_2 (black trace), SnO_2 (red trace) and ZrO_2 films (blue trace). Inset is a scheme showing (1) photoinduced electron injection into TiO_2 and (2) recombination between conduction-bandelectrons of TiO_2 and oxidized nanocrystals. Reprinted with permission from Leventis et al. (2010). (For interpretation of the references to color in this figure legend, the reader is referred to the web version of this article.)

be achieved only for very small size ($\sim d = 3$ nm) PbS QDs (Acharya et al., 2010). Considering that there are lots of unexplored combinations of QDs materials and hole conducting polymers we could conclude that this device architecture is promising and future research is needed in this direction.

7. Bulk heterojunction (polymer) solar cells

Bulk heterojunction photovoltaics have been intensively studied during the last decade due to their compatibility with low-temperature roll-to-roll manufacturing (Hoppe and Sariciftci, 2004). Bulk heterojunction devices are composed of electron-donating conjugated polymers and electron-accepting fullerenes. The performance of these cells has steadily improved, with conversion efficiencies approaching 6.1% (100 mW/cm^2, AM 1.5G) (Park et al., 2009). However, for large scale commercialization the efficiencies of these devices need to be further improved. Integration of semiconductor nanoparticles in bulk heterojunction solar cells is believed to provide an alternative ways to further boost the efficiencies of these devices (Han et al., 2006;). Up to now various semiconductor nanomaterials such as TiO_2 (Lin et al., 2009), $ZrTiO_4$/Bi_2O_3 (Hussain et al., 2010), ZnO (Lloyd et al., 2009), ZnS (Bredol et al., 2009), CdS (Jiang et al., 2010), CdSe (Arango et al., 2009), CdTe (Shiga et al., 2006), PbS (Maria et al., 2005), PbSe (Tan et al., 2009), Si (Liu et al., 2009) and etc. have been used in bulk heterojunction solar cells. The research on QDs in bulk heterojunction devices focuses on two aspects. Firstly, QDs are used in bulk heterojunction devices in the presence of electron transporting fullerenes and hole conducting polymers (Feng et al., 2010; Arenas et al., 2010; Chen et al., 2008). QDs are added in the fullerene/polymer composite as light harvesting material. Secondly, QDs are used in bulk heterojunction solar cells as light harvesting and simultaneously as electron transporting material (Wang et al., 2010a; Zhou et al., 2010). In the latter configuration the fullerenes are omitted as electron conducting phase. Fig. 10 illustrates a scheme of a typical bulk heterojunction device composed of CdSe nanorods and hole conducting polymer PCPDTBT (Dayal et al., 2010a). Here the CdSe nanorods are used as electron acceptor material while PCPDTBT is used as donor phase. Unlike the polymer/fullerene bulk heterojunction cells where the fullerene contributes very little to the spectral response, the QDs based polymer solar cells offer an advantage for efficient light absorption. Current researches on QDs based bulk heterojunction solar cells are focused on several important points like: studies of phase segregation between the donor and the acceptor layers, studies to achieve controlled agglomeration of semiconductor nanocrystals in the polymer films, loading amount of nanocrystals in the polymer films, studies concerning the shape of the used nanocrystals, researches related to surface modifications of nanocrystals and finally studies which deal with new combinations of nanocrystals and polymers. In comparison to the fullerene/polymer system where the main point lies in the phase separation of the two components, in QDs based polymer solar cells this limitation could be overcome by appropriate surface treatment of the nanocrystals (Fig. 10c) (Xin et al., 2010; Lokteva et al., 2010; Truong et al., 2010). It has been shown that the photoconversion efficiencies of these devices depend on the

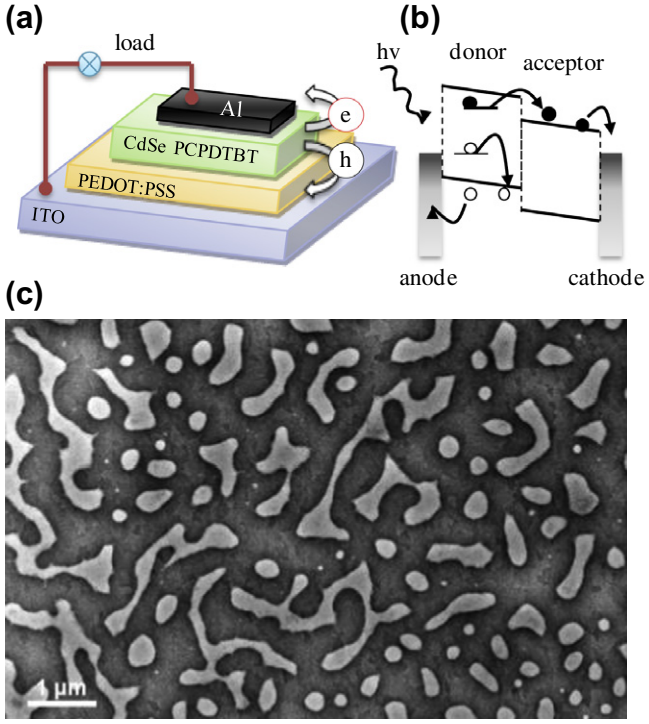

Fig. 10. (a) Scheme of a bulk heterojunction device. (b) Energy diagram of a typical device architecture and (c) SEM image from a composite of CdSe QDs and P3HT. Light and dark areas in (c) are due to phase segregation. Taken with permission from De Girolamo et al. (2007).

nanocrystal shape. For example, devices composed of rod shape nanoparticles show better efficiencies than nanoparticles with spherical geometry due to improved inter-particle hops for the electrons in the case of rods (Sun et al., 2003; Wang et al., 2006, 2010b). Beside the shape of the QDs, loading amount of the nanoparticles in the films also plays a major role for efficient charge transport (Albero et al., 2009). The hole transporting polymers also play significant role in the charge transport process. Fig. 11 shows typical hole conducting polymers used in bulk heterojunction solar cells.

One of the earliest reports on bulk heterojunction solar cells was made by Alivisatos group for the system with CdSe QDs and polymer MEH-PPV (Greenham et al., 1996, 1997). Initially these devices gave very low power conversion efficiencies in the order of 0.1% (80 mW/cm^2, AM 1.5). However, in later studies conducted by the same group the polymer MEH-PPV was replaced with P3HT (Huynh et al., 1999; Huynh et al., 2002, 2003). Simultaneously they studied CdSe spherical, rod and tertrapod shape structures in those devices. As an example CdSe rods in combination with P3HT in heterojunction devices demonstrated a power conversion efficiency in the order of 1.7%, a $J_{SC} = 5.7$ mA/cm^2, a $V_{OC} = 0.7$ V and a FF = 40% (100 mW/cm^2, AM 1.5). Furthermore, rods were found to be superior to spheres allowing better carrier transport and consequently yielding higher conversion efficiencies. Fig. 12 shows TEM images of typical CdSe nanocrystals used in photovoltaic studies. On the other hand it

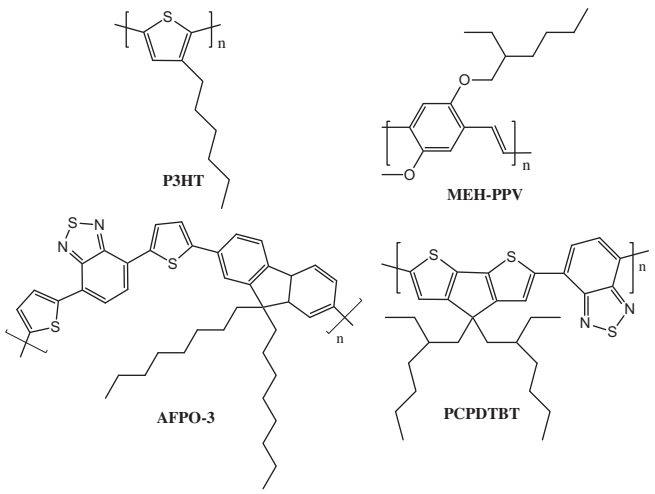

Fig. 11. Schematic illustrations of various hole conducting polymers. P3HT: poly(3-hexylthiophene); MEH-PPV: poly[2-methoxy-5-(2′-ethylhexyloxy)-1,4phenylenevinylene; AFPO-3: poly[2,7-(9,9-dioctyl-fluorene)-*alt*-5,5-(4′,7′-di-2-thienyl-2′,1′,3′-benzothiadiazole)]; PCPDTBT: poly[2,6-(4,4-bis-(2-ethylhexyl)-4*H*-cyclopenta[2,1-*b*;3,4-*b*′]dithiophene)-*alt*-4,7-(2,1,3-benzothiadiazole)].

seems that not only the shape of the nanocrystals affect the charge transport but also the specific aggregation of QDs in the polymer films. Zhou et al. (2010) recently showed that chemical treatment of CdSe QDs can improve their aggregation. Due to this aggregation in the polymer films a facilitated electron transport across the QDs layer could be achieved (Huang et al., 2008). Fig. 13 shows current–voltage characteristics from a typical device composed of CdSe QDs and P3HT polymer. Further, control over the QDs aggregation can be achieved by surface modification of the nanocrystals. Olson et al. (2009) studied blends of CdSe QDs and P3HT polymer in the presence of various capping ligands. Their findings show that the devices fabricated after butylamine treatment give enhanced photoconversion efficiencies. Similarly, Palaniappan et al. (2009) studied the influence of functional groups of P3HT in CdSe QDs blends. They found that mercapto-P3HT modified CdSe nanoparticles give better performances. Molecular modification of QDs is demonstrated to be successful by De Girolamo et al. (2007) as well. The employed methodology which is based on molecular recognition process between 1-(6-mercaptohexyl)thymine functionalized CdSe QDs and P3HT. By using this strategy they achieved phase segregation on a micrometer scale between the donor and the acceptor materials. Moreover, the degree of phase segregation can be controlled by the employed solvents where donor and acceptor materials are dissolved. Sun and Greenham (2006) studied the effect of solvent on phase formation between CdSe nanorods and P3HT polymer. By using 1,2,4-trichlorobenzene solvent they achieved control over the morphology (achieved fibrous structure) of P3HT films. Blends of CdSe nanorods and P3HT used to fabricate these photovoltaic devices gave solar conversion efficiencies of about 2.6% (92 mW/cm^2, AM1.5). Table 1 shows the efficiencies of the most successful heterojunction devices consisting of CdSe nanoparticles and various hole conducting polymers. Comparing the photoconversion

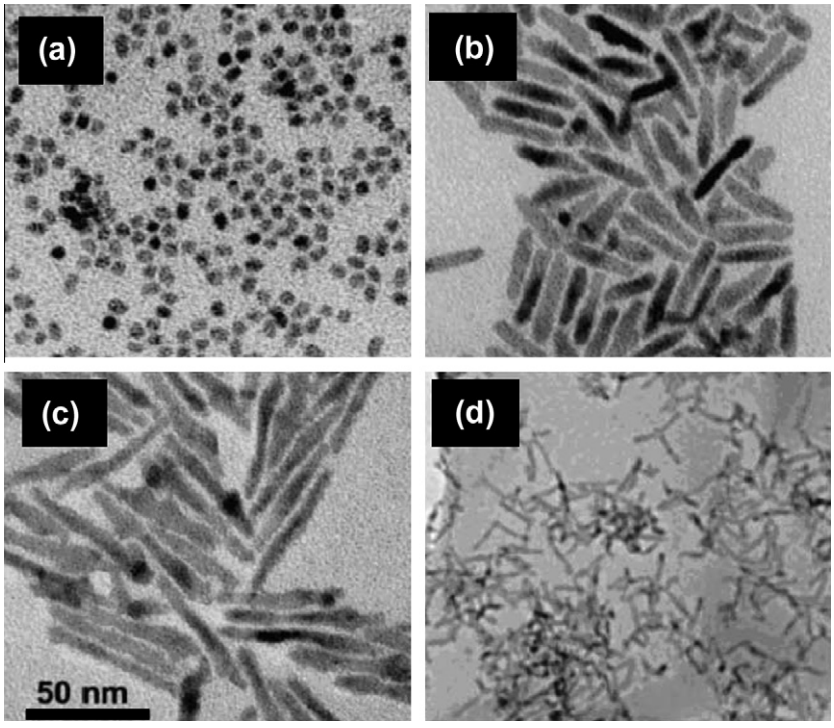

Fig. 12. TEM images of CdSe nanocrystals with different shapes: (a) nanospheres, (b) smaller aspect ratio nanorods, (c) larger aspect ratio nanorods and (d) tetrapods. Reprinted with permission from Huynh et al. (2002) and Dayal et al. (2010b).

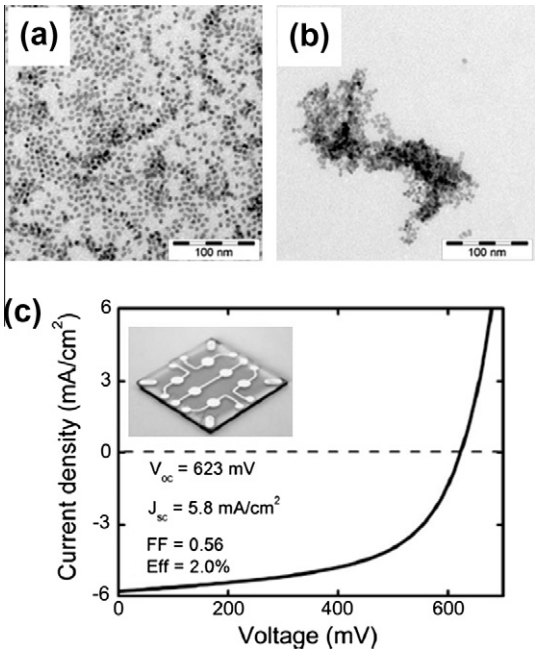

Fig. 13. TEM images of CdSe QDs (a) without and (b) with chemical treatment (see the text). (c) Current–voltage characteristic of CdSe/P3HT cell under illumination (100 mW/cm^2). The scale bars in the top images correspond to 100 nm. The inset in (c) is a typical photovoltaic device. Reprinted with permission from Zhou et al., (2010).

efficiencies for CdSe QDs and P3HT it seems that the results are greatly affected by the preparation methods. This deviation might be caused due to oxidation of the nanocrystals by molecular oxygen or low quality of the used CdSe nanocrystals. Besides P3HT polymer, it was demonstrated that there are other hole conducting polymers such as APFO-3 which also gave promising results in CdSe QDs heterojunction devices (Wang et al., 2006).The photovoltaic device prepared from this blend showed a spectral response exceeding 650 nm and yielding a power conversion efficiency of 2.4% (100 mW/cm^2, AM 1.5).

In recent years, much research efforts have been focused on lead chalcogenide nanocrystals due to the fact their absorbance extend in the near-infrared region, NIR (Wang et al., 2008; Seo et al., 2009; Noone et al., 2009). Despite the active research on bulk heterojunction devices with PbS and PbSe nanoparticles the reported efficiencies for this materials are still below that of CdSe nanoparticles. Jiang et al. (2007) demonstrated that devices composed of PbSe QDs in combination with P3HT showed

Table 1
Photoconversion efficiencies of bulk heterojunction devices composed of CdSe nanocrystals and various hole conducting polymers.

Nanocrystals	Polymers	Eff. (%)	References
CdSe dots	P3HT	1.8	Olson et al. (2010)
CdSe dots	P3HT	2.0	Zhou et al. (2010)
CdSe dots	P3HT	2.6	Sun and Greenham (2006)
CdSe tetrapods	APFO-3	2.4	Wang et al. (2006)
CdSe tetrapods	PCPDTBT	3.1	Dayal et al. (2010b)

$J_{SC} = 1.08$ mA/cm^2, $V_{OC} = 0.37$ V, FF = 37% and power conversion efficiencies of 0.14% (100 mW/cm^2 AM 1.5). To the best of our knowledge, by using PbS and PbSe QDs the highest achieved power conversion efficiency stand at 0.55% with a $J_{SC} = 4.2$ mA/cm^2, a $V_{OC} = 0.38$ V and FF = 34% (AM 1.5) (Noone et al., 2010). In conclusion achieving efficient photon-to-current conversion in bulk heterojunction devices will require: (i) controlled aggregation of semiconductor nanoparticles in the polymer film, (ii) surface modification of the nanocrystals, (iii) and selecting new materials with near-infrared response as well as utilizing new hole conducting polymers.

8. Quantum dot sensitized solar cells

8.1. Working mechanism

The earliest work on quantum dot sensitized solar cells (QDSSCs) has been reported by Weller's group (Vogel et al., 1990). These types of solar cells are alternative to dye sensitized solar cells (DSSCs) (Mishra et al., 2009). The difference between QDSSCs and DSSCs lies in the sensitizer employed to harvest the sun light. In the case of DSSCs this is an organic dye molecule or metal–organic complex whereas in the case of QDSSCs it is an inorganic semiconductor material QDs. Fig. 14 shows a scheme of quantum dot sensitized solar cell and its principle of operation. Briefly the working principle of QDSSCs is as follows: Upon illumination of the photovoltaic cell the QDs sensitizer attached on the TiO_2 film absorb incident light. This causes excitation of an electron in QDs from the valence band to the conduction band. In this way the excited electron leave behind a positive hole. The electrostatically bound electron–hole pair called an exciton undergoes dissociation at the QDs/TiO_2 interface. The excited electrons are injected into the TiO_2 nanoporous electrode, resulting in the oxidation of the QDs photosensitizer. Further, the injected electrons in TiO_2 are transported through the external load to the counter electrode. Meanwhile, the oxidized QDs accept electrons from redox mediator regenerating the ground state of QDs sensitizer. Consequently, the oxidized mediator diffuses to the counter electrode

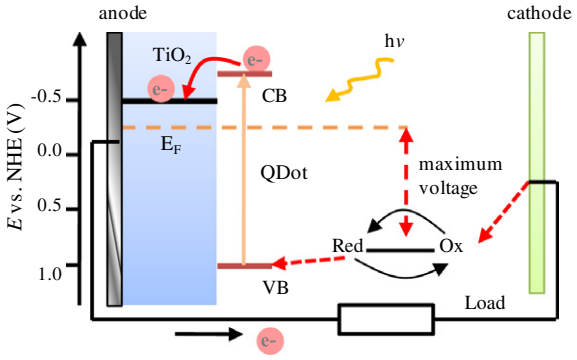

Fig. 14. Scheme of a QDsSSC and its working mechanism.

where it is reduced. In this way one cycle is completed and the gained power is due to the absorbed photons by semiconductor nanocrystals.

8.2. Sensitization of TiO_2 electrodes with QDs

Metal oxides of wide band-gap semiconductors such as TiO_2 and ZnO have been the most often used porous electrodes in QDSSCs. Morphologies of these metal oxides have been actively explored in order to achieve maximum power conversion efficiencies from these devices (Yum et al., 2007; Lee et al., 2008b; Toyoda et al., 2007; Baker and Kamat, 2009; Chen et al., 2006; Liu et al., 2010a). For example, nanowires of metal oxides were used in order to increase the conductivity of the films (Chen et al., 2010a). Similarly, nanotubes of metal oxides were used in order to enhance the carrier transport and achieve light trapping effect. Inverse opal structures have been used for the same purpose as well. Fig. 15 shows typical morphologies of TiO_2 and ZnO films employed in the preparation of QDSSCs.

Sensitization of metal oxides with nanocrystals have been focused on four approaches: (i) QDs have been grown directly onto TiO_2 electrodes using chemical bath deposition (CBD) procedure (Toyoda et al., 2007); (ii) successive ion-layer adsorption and reaction (SILAR) procedure (Chang and Lee, 2007; Lee et al., 2009b, 2010); (iii) QDs have been attached to metal oxide surfaces through bi-functional linkers (Robel et al., 2006; Sambur and Parkinson, 2010; Sambur et al., 2010), and (iv) QDs have been linked to metal oxides using physisorption process (Giménez et al., 2009; Blackburn et al., 2005).

Chemical bath deposition is the earliest method applied for deposition of semiconductor QDs on metal oxide surfaces (Šimurda et al., 2006). This method gained popularity because of its simplicity and possibility to apply it in large scale production. However, despite its simplicity in general chemical bath deposition does not allow precise control over the particle size distribution and spectral properties of QDs. In recent years chemical bath deposition method has transformed into a more successful technique called successive ion-layer adsorption and reaction method (SILAR). Simultaneously, another method that gained also wide recognition is the linker assisted self assembly. In this procedure pre-synthesized nanocrystals are adsorbed on metal oxides surface by using molecular linkers that have various functional groups. Linker assisted self assembly enables, in principle, a precise control over the spectral properties of QDs and the interconnectivity between QDs and the substrate surface, while ensuring monolayer surface coverage. Less unexplored procedure that received attention during the past several years is based on physisorption. In this method sensitization of metal oxides is achieved through physisorption. Usually bare metal oxide electrodes are dipped into solutions of QDs with the immersion time reaching 100 h. Moreover, the sensitized electrodes with QDs are assembled into photovoltaic cells and the obtained results suggest that the sensitization by this procedure is much better than using bi-functional linkers.

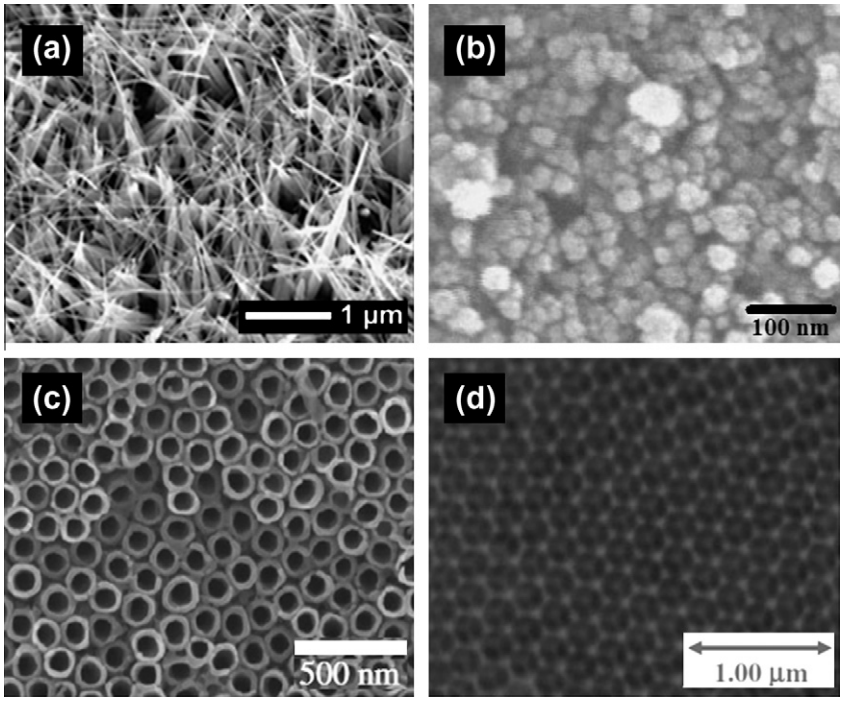

Fig. 15. SEM images of TiO_2 and ZnO films with various morphologies: (a) nanowires; (b) mesoporous structures; (c) nanotubes and (d) inverse opal. Data are reproduced with permission from Chen et al. (2010a), Lee et al. (2008b) and Toyoda et al. (2007).

8.3. CBD and SILAR

Semiconductor QDs such as CdS (Peter et al., 2002; Lin et al., 2007), CdSe (Diguna et al., 2007), PbS (Hoyer and Könenkamp, 1995), CdS(core)/CdSe(shell) (Chen et al., 2006) and InP (Zaban et al., 1998) have been actively used in quantum dot sensitized solar cell. They have been often assembled onto porous TiO_2 films by using CBD or SILAR methods. In the CBD approach, dissolved cationic and anionic precursors reacts slowly in one bath (Niitsoo et al., 2006; Toyoda et al., 2008; Okazaki et al., 2007). In this way by varying the reaction time it is possible to control the deposition rate of QDs. Simultaneously, the growth of QDs have been evaluated by separating the cationic and anionic precursors into two beakers and dipping the bare electrodes alternatively into each beaker (Pathan and Lokhande, 2004; Lee et al., 2009a). This so called SILAR process has been initially used for preparation of CdS and PbS QDs sensitized electrodes. Recently, it has been extended for the preparation of CdSe and CdSe(Te) QDs sensitized TiO_2 electrodes (Lee et al., 2008c). In both principle and practice, the SILAR process could now be considered better than CBD for deposition of QDs layers onto mesoporous oxides.

One of the most studied materials in photolectrochemical cells is CdS (Zhu et al., 2010; Gao et al., 2009). The reason for its widespread use lies in the fact that CdS QDs can be easily prepared and can be used in aqueous solution with polysulfide redox mediator. However, the photoconversion efficiencies obtained from this material are usually low due to its absorption range which is limited to wavelength below 550 nm (Grätzel, 2001). Since photogenerated current is proportional to the optical absorption it is much useful to use lower band-gap semiconductors. For this purpose semiconductors like CdX (X = Se, Te) or PbS are often employed in QDSSCs. Diguna et al. (2007) demonstrated that CdSe QDs grown *in situ* on TiO_2 inverse opal show a power conversion efficiency of about 2.7% (100 mW/cm^2). This efficiency is much higher than 1.6% reported for CdS QDSSCs (Zhang et al., 2010). Furthermore, Fan et al. (2010) showed that the performance of CdSe QDSSCs can be greatly influenced by the counter electrode as well. Their photovoltaic devices composed of carbon electrode has demonstrated an IPCE = 80%, a $J_{SC} = 12.41$ mA/cm^2, a $V_{OC} = 0.6$ V, an FF = 52% and a power conversion efficiency reaching 3.9% (100 mW/cm^2, AM 1.5). In other studies co-sensitization of TiO_2/CdS with CdSe QDs was found to be an alternative way to improve the power conversion efficiencies (Niitsoo et al., 2006; Sudhagar et al., 2009; Wang et al., 2010c). Moreover, sensitization of TiO_2 electrodes with narrow band-gap materials such as CdTe (Wang et al., 2010b) and PbS QDs (Lee et al., 2009a,c,d) have also been demonstrated to be promising in QDSSCs. However, the most common polysulfide (S^{2-}/S_2^{2-}) electrolyte used for CdS and CdSe QDs is not the best choice for low band-gap materials. For example, in the presence of S^{2-} ions CdTe QDs undergoe anodic corrosion (Bang and Kamat, 2009). To avoid unwanted photocorrosion processes in low band-gap materials cobalt complexes are used as redox mediators (Sapp et al., 2002). The role of redox mediators in QDSSCs will be discussed in next sub-chapters.

8.4. Linker-assisted assembly

A key issue governing efficient electron transfer between two semiconductors is interfacial electronic energy alignment. The ability to tune electronic energy alignment of QDs allows one to optimize the band positions for efficient photon-to-current conversion (Schaller and Klimov, 2004; Carlson et al., 2008; Shen and Lee, 2008). Currently there are four approaches available for modulation of interfacial electron transfer. The first approach is studied in detail by Watson and coworkers and provides evidence that the nature of linker molecules between CdS QDs and TiO_2 nanoparticles influences the kinetics and efficiency of excited-state interfacial electron transfer (Dibbell and Watson, 2009). Moreover, they used bifunctional linker molecules that belong to the type X-R-Y, where X and Y are groups that bind to CdSe (X = SH) and TiO_2 (Y = COOH), respectively. The second approach is based on evaluation of size dependent electron transfer rates (Tvrdy and Kamat, 2009; Robel et al., 2007). It was found that the electron injection rate from CdSe QDs to TiO_2 depends on the size of CdSe QDs. Controlling CdSe QDs size therefore provides a convenient way to modulate the band-gap energies. In the third approch, an alternate way to modulate the electron injection rate is to tune the band edge of TiO_2 (Fig. 16). It has been established that pH induced protonation of surface groups is useful to shift the band edge of TiO_2 (Tomkiewicz, 1979; Bolts and Wrighton, 1976; Chakrapani et al., 2010). In comparison to dye molecules, the QDs are ideal to study pH driven electron transfer kinetics due to the robustness of the QDs bands toward pH increase. The fourth strategy which is used to enhance the photoconversion efficiencies is based on molecular modification of semiconductor surfaces (Cahen and Khan, 2003). It was demonstrated that molecular grafting is powerful in tuning the energy levels of QDs. Barea et al., showed that molecular dipoles attached on QDs can control both injection and recombination in QDSSCs (Barea et al., 2010).

Sensitization of TiO_2 electrodes with pre-synthesized QDs was actively studied during the recent years (Mann and Watson, 2007; Lee et al., 2008a–d; Sambur and Parkinson, 2010a; Sambur et al., 2010b). It was demonstrated that mercaptopropionic acid allows good connection between QDs and mesoporous TiO_2 films (Chen et al., 2009a; Prabakar et al., 2010; Lee et al., 2007). Recently, Chen et al. (2009b) showed that pre-synthesized CdS QDs can be effectively attached on TiO_2 electrodes by using this linker. The as prepared CdSe QDSSCs showed photoconversion efficiencies in the order of 1.19% (100 mW/cm^2). Moreover, this binding strategy was proven to be

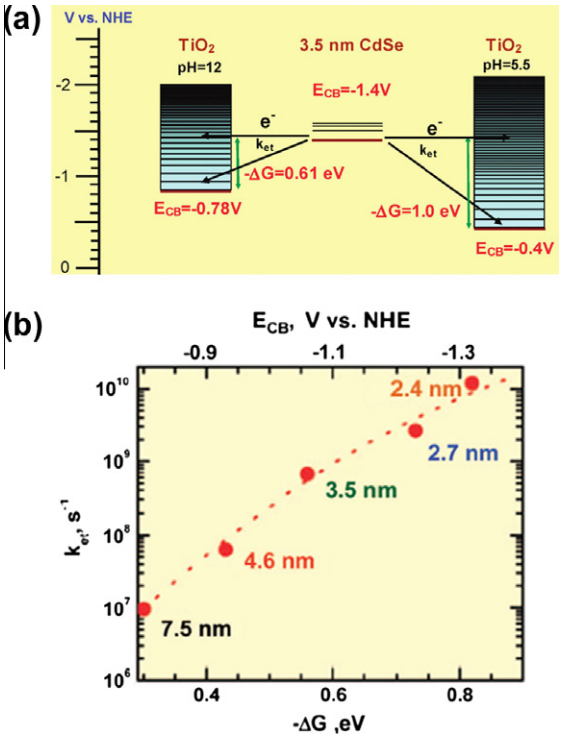

Fig. 16. (a) Scheme describing the shift (ΔG) in the conduction-bandof TiO_2 at different pH conditions. (b) Electron transfer rate versus ΔG. Data are taken with permission from Chakrapani et al. (2010) and Robel et al. (2007).

effective for sensitization of one-dimensional (1D) semiconductors nanowires made of TiO_2 and ZnO. Photoelectrodes are developed in which arrays of nanowires are grown vertically onto a conducting substrate present alternative to the mesoporous electrodes. Leschkies et al. (2007) used CdSe QDs and ZnO nanowires to develop a new QDSSCs architecture. By using CdSe sensitized ZnO nanowire QDSSCs they measured 0.4% power conversion efficiency (100 mW/cm^2).

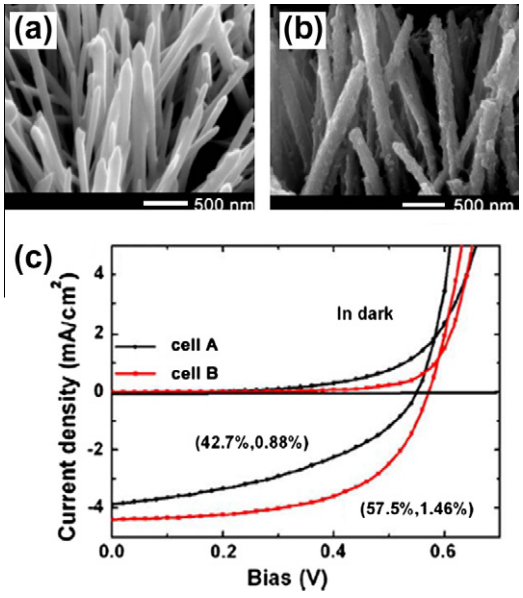

Fig. 17. SEM images of: (a) CNT/ZnO and (b) CNT/ZnO/CdSe QDs. (d) Current–voltage characteristics of CNT/ZnO/CdSe QDs photovoltaic cells at illumination 1 sun (100 mW/cm^2). Data are taken with permission from Chen et al. (2010b).

Integration of carbon nanotubes into TiO_2 provide favorable charge collection at the ITO electrode (Lee et al., 2008d; Farrow and Kamat, 2009). Based on these results Chen et al. (2010b), developed QDSSCs consisting of vertically aligned carbon nanotubes (VACNT), ZnO nanowires and CdSe QDs. Due to inhibited charge recombination at the ZnO surface (or CdSe) a power conversion efficiency of 1.46% is achieved (100 mW/cm^2, AM 1.5). Fig. 17 shows typical current–voltage curves and morphology of the used ZnO nanowires. This system gives hints that in future researches the integration of carbon nanotubes/metal oxide composites will play an important role in QDSSCs.

Efficient light harvesting often require sensitizer QDs that absorb light in the NIR. For this purpose CdTe and CdHgTe QDs have been found ideal in QDSSCs (Lan et al., 2009; Gao et al., 2009). Yang and Chang (2010) reported for CdHgTe QDSSCs a power conversion efficiency of about 2.2%, a $J_{SC} = 4.43$ mA/cm^2, a $V_{OC} = 0.71$ V and an IPCE = 18% (100 mW/cm^2, AM 1.5). The low IPCE could be attributed to the loading amount of QDs in the TiO_2 electrode or inefficient electron injection from the QDs to the TiO_2 film. In addition the reported photocurrent efficiencies of QDSSCs by using linker assisted method are lower than those for QDSSCs obtained using the SILAR method. Nevertheless, this procedure allows evaluation of size dependent electron transfer rates in QDs/metal oxide electrodes which could be difficult to estimate with other methods.

8.5. Surface states and back electron transfer

Despite the active research on QDSSCs the performances of these devices are still low compared with DSSCs. The low efficiencies of QDSSCs are often attributed to QDs surface states or back electron transfer that may occur at the solid–liquid interface (Shalom et al., 2009; Hodes, 2008). The surface states sometimes called trap states may interfere with electron injection from QDs into TiO_2. Fig. 18 illustrates the various pathways where an excited electron undergoes after illumination. These are as follows: (a) recombination with the holes left behind after illumination, (b) recombination through surface states or (c) recombination with redox mediator. Passivation of surface states is often achieved by molecular modification or deposition of a second semiconductor material. For example it is known that a thin layer of ZnS on CdSe is useful to remove the surface states (dangling bonds) in the QDs. Similarly, passivation can be achieved with a dense TiO_2 layer on top of the QDs (Diguna et al., 2007). Furthermore, surface passivation can also be achieved with organic molecules as well (Barea et al., 2010). In designing efficient inorganic coating materials it is recommended to take into account the lattice mismatch between the two semiconductor materials.

8.6. The role of redox mediator in QDSSCs

In dye sensitized solar cells, platinum (Pt) is commonly used as a counter electrode and I^-/I_3^- as redox couple. This reason is due to the stability and catalytic activity of Pt for reduction of I_3^-. Unfortunately, the well-known I^-/I_3^- redox couple is not compatible with low band-gap semiconductor materials, leading to a rapid corrosion process of the semiconductors. This redox couple was tested in CdS and CdSe QDSSCs while the corrosive reaction was observed to progress gradually (Rühle et al., 2010). For QDSSCs alternative redox couples based on polypyridyl cobalt complexes, $[\text{cobalt(o-phen)3}]^{2+/3+}$ (Sapp et al., 2002), ferrocene/ferrocenium (Tachibana et al., 2008) and polysulfide (S^{2-}/S_x) appear to work quite well (Tachibana et al., 2007). Furthermore, the cobalt(II/III) complexes were demonstrated to be efficient redox mediators for low band-gap semiconductor materials such as InAs, InP or PbS QDs. However, there are certain drawbacks of cobalt redox mediators in QDSSCs as well. While the cobalt redox mediators give relatively good photoconversion efficiencies at low illuminations (0.1 sun) they fail at high illuminations (1 sun). The latter is explained with the low diffusion mass transport of cobalt complexes.

8.7. Three-electrode cell

The measurement and calibration of current–voltage curves sometime require caution. The measurements are usually executed with two or three-electrode system. Evaluation of real photovoltaic parameters by using three-electrode system appears to be not straightforward because of the irreversible character of the redox reaction used to regenerate the sensitizer. By using reversible redox mediators, the utilization of three-electrode cell overestimates the conversion efficiency, since diffusion and electron transfer overvoltage losses are neglected (Sun et al., 2008). In the meantime, the current–voltage data obtained in the three-electrode system should be referenced versus the dark potentials. Besides the three-electrode systems it is recommended to obtain the voltammograms independently with a two electrode system.

8.8. The role of counter electrode in QDSSCs

The choice of counter electrode is one of the essential points in achieving efficient photoconversion. Because the counter electrode controls the regeneration of oxidized mediator into its reduced form it is vital to select a counter electrode with low charge resistance. Since, polysulfide (S^{2-}/S_x^{2-}) redox mediator is often used in QDSSCs, this require replacement of the commonly employed Pt counter electrode with other electrodes. Polysulfide redox mediator is often used in combination with platinum (Pt), gold (Au), carbon (C) and copper sulfide (Cu_2S) counter electrodes. Among these materials carbon is ideal alternative to Pt electrodes, due to the fact that it allows catalytic activity and

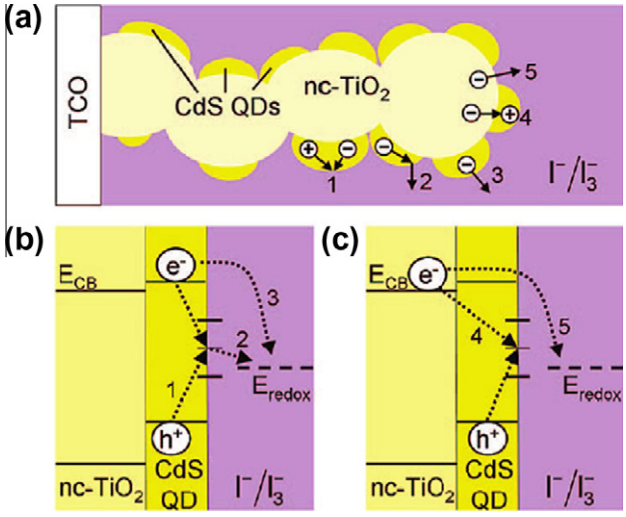

Fig. 18. (a) Schematic drawing of CdS QDs sensitized TiO_2 electrodes. Various paths for electrons are shown with arrows. (b) Energy diagram showing the path for excited electrons in CdSe QDs to surface states (1) or transfer to oxidized species, I_3^-, via direct path (3) and via surface states (2). (c) Energy diagram showing the recombination of excited electrons in TiO_2 with holes at surface states (4) or transfer to oxidized species, I_3^-, via direct path (5). Reprinted with permission from Shalom et al. (2009).

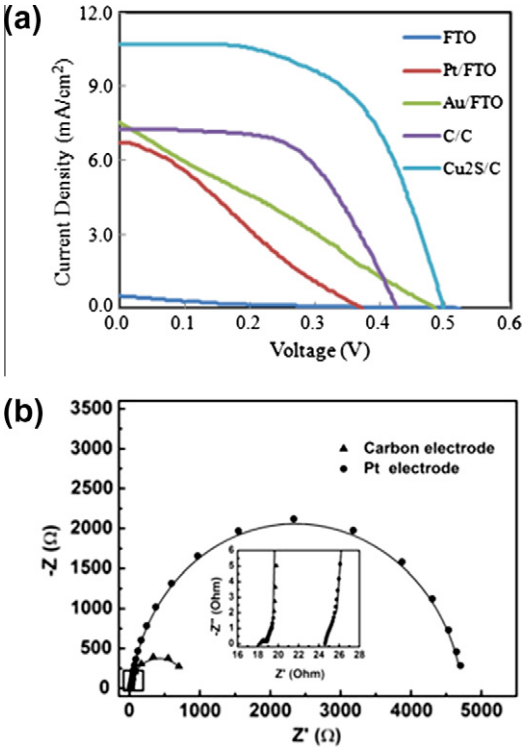

Fig. 19. Current–voltage characteristics (a) and Nyquist plots (b) for QDSSCs with different counter electrodes. The data in (a) are digitalized with getdata draph digitazier from Deng et al. (2010). The scattered points in (b) are experimental data and the solid lines are the fitting curves. The data in (b) are taken with permission from Zhang et al. (2010).

sufficient conductivity. Furthermore, carbon electrodes can be prepared in the form of mesoporous material which can effectively increase the electron transfer rate for reduction of S_2^{2-} ions (Fan et al., 2010). Fig. 19 shows current–voltage

characteristics and impedance plots of CdS/CdSe QDSSCs of various counter electrodes. Reduced sheet and charge transfer resistances makes the carbon electrode ideal in QDSSCs. Recently, Mora-Seró et al. (2008) evaluated that Pt counter electrode constituted a limiting factor for the cell performance because of strong adsorption of sulfides ions onto Pt surface, which impair its catalytic activity. Similarly, Lee and Lo (2009) demonstrated that Au counter electrode in CdS/CdSe QDSSCs is more immune to sulfur ions than Pt giving higher conversion efficiencies in the order of 4.2% (100 mW/cm^2). In addition, Zhang et al. (2010) demonstrated that the efficiency of CdS photovoltaic devices can be increase from 0.13% up to 1.47% just by replacing the Pt with carbon counter electrode. In a recent study Cu_2S counter electrode was also found to give high efficiencies. Shen et al. (2010) used this material in CdSe QDSSCs and achieved photoconversion efficiency of about 1.8% (100 mW/cm^2). Furthermore, Meng's group employed combined Cu_2S/carbon counter electrode in CdS/CdSe QDSSCs and reported an efficiency of 3.1% (100 mW/cm^2) (Deng et al., 2010). In the meantime, this composite counter electrode was superior to the commonly used Pt, Au and carbon electrodes. In addition, electrodes with low sheet and low charge transfer resistance improve greatly the photoconversion efficiencies.

9. Conclusions

Here we reviewed the recent advances in utilizing colloidal quantum dots as light harvesters in various types of photovoltaic devices. At present the power conversion efficiencies of colloidal quantum dot solar cells are about 5%. Further research is needed in this area to screen potential systems which could provide a roadmap for the design of super efficient solar cells. Development of high performance photovoltaic cells will necessitate the use of high quality nanocrystals with good material properties. In achieving this goal surface state of the nanocrystals should be well passivated. This could be achieved either by using organic or inorganic capping ligands. In conclusion, well ordered semiconductor nanoparticles in photovoltaic cells are tought to bring a major breakthrough in this field.

References

Acharya, K.P., Hewa-Kaskarage, N.N., Alabi, T.R., Nemitz, I., Khon, E., Ullrich, B., Anzenbacher, P., Zamkov, M., 2010. Synthesis of PbS/TiO_2 colloidal heterostructures for photovoltaic applications. J. Phys. Chem. C 114, 12496–12504.

Albero, J., Martínez-Ferrero, E., Ajuria, J., Waldauf, C., Pacios, R., Palomares, E., 2009. Photo-induced electron recombination dynamics in CdSe/P3HT hybrid heterojunctions. Phys. Chem. Chem. Phys. 11, 9644–9647.

Arango, A.C., Oertel, D.C., Xu, Y., Bawendi, M.G., Bulović, V., 2009. Heterojunction photovoltaics using printed colloidal quantum dots as a photosensitive layer. Nano Lett. 9, 860–863.

Arenas, M.C., Mendoza, N., Cortina, H., Nicho, M.E., Hu, H., 2010. Influence of poly3-octylthiophene (P3OT) film thickness and preparation method on photovoltaic performance of hybrid ITO/CdS/P3OT/Au solar cells. Sol. Energy Mater. Sol. Cells 94, 29–33.

Arici, E., Sariciftci, N.S., 2004. Hybrid solar cells. In: Nalwa, H.S. (Ed.), . In: Encyclopedia of Nanoscience and Nanotechnology, vol. 3. American Scientific Publishing, pp. 929–944.

Bang, J.H., Kamat, P.V., 2009. Quantum dot sensitized solar cells. A tale of two semiconductor nanocrystals: CdSe and CdTe. ACS Nano 3, 1467–1476.

Barea, E.M., Shalom, M., Giménez, S., Hod, I., Mora-Séro, I., Zaban, A., Bisquert, J., 2010. Design of injection and recombination in quantum dot sensitized solar cells. J. Am. Chem. Soc. 132, 6834–6839.

Baker, D., Kamat, P., 2009. Photosensitization of TiO_2 nanotubes with CdS quantum dots: Particulate versus tubular support architectures. Adv. Funct. Mater. 19, 805–811.

Beard, M., Knutsen, K., Yu, P., Luther, J., Song, Q., Metzger, W., Ellingson, R., Nozik, A., 2007. Multiple exciton generation in colloidal silicon nanocrystals. Nano Lett. 7, 2506–2512.

Blackburn, J.L., Selmarten, D.C., Ellingson, R.J., Jones, M., Micic, O., Nozik, A.J., 2005. Electron and hole transfer from indium phosphide quantum dots. J. Phys. Chem. B 109, 2625–2631.

Bolts, J.M., Wrighton, M.S., 1976. Correlation of photocurrent–voltage curves with flat-band potential for stable photoelectrodes for the photoelectrolysis of water. J. Phys. Chem. 80, 2641–2645.

Bredol, M., Matras, K., Szatkowski, A., Sanetra, J., Prodi-Schwab, A., 2009. P3HT/ZnS: a new hybrid bulk heterojunction photovoltaic system with very high open circuit voltage. Sol. Energy Mater. Sol. Cells 93, 662–666.

Cahen, D., Khan, A., 2003. Electron energetics at surfaces and interfaces: concepts and experiments. Adv. Mater. 15, 271–277.

Carlson, B., Leschkies, K., Aydil, E., Zhu, X.-Y., 2008. Valence band alignment at cadmium selenide quantum dot and zinc oxide (1 0 0) interfaces. J. Phys. Chem. C 112, 8419–8423.

Chakrapani, V., Tvrdy, K., Kamat, P.V., 2010. Modulation of electron injection in CdSe–TiO_2 system through medium alkalinity. J. Am. Chem. Soc. 132, 1228–1229.

Chang, C.-H., Lee, Y.-L., 2007. Chemical bath deposition of CdS quantum dots onto mesoscopic TiO_2 films for application in quantum-dot-sensitized solar cells. Appl. Phys. Lett. 91, 053503.

Chang, J.A., Rhee, J.H., Im, S.H., Lee, Y.H., Kim, H.-J., Seok II, S., Nazeeruddin, M.K., Grätzel, M., 2010. High-performance nanostructured inorganic–organic heterojunction solar cells. Nano Lett. 10, 2609–2612.

Chen, S., Paulose, M., Ruan, C., Mor, G.K., Varghese, O.K., Kouzoudis, D., Grimes, C.A., 2006. Electrochemically synthesized CdS nanoparticle-modified TiO_2 nanotube-array photoelectrodes; preparation, characterization, and application to photoelectrochemical cells. J. Photochem. Photobiol. A 177, 177–184.

Chen, H.-Y., Lo, M.K.F., Yang, G., Monbouqette, H.G., Yang, Y., 2008. Nanoparticle-assisted high photoconductive gain in composites of polymer and fullerene. Nat. Nanotechnol. 3, 543–547.

Chen, J., Song, J.L., Sun, X.W., Deng, W.Q., Jiang, C.Y., Lei, W., Huang, J.H., Liu, R.S., 2009a. An oleic acid-capped CdSe quantum-dot sensitized solar cell. Appl. Phys. Lett. 94, 153115.

Chen, J., Zhao, D.W., Song, J.L., Sun, X.W., Deng, W.Q., Liu, X.W., Lei, W., 2009b. Directly assembled CdSe quantum dots on TiO_2 aqueous solution by adjusting pH value for quantum dot sensitized solar cells. Electrochem. Commun. 11, 2265–2267.

Chen, J., Wu, J., Lei, W., Song, J.L., Deng, W.Q., Sun, X.W., 2010a. Co-sensitized quantum dot solar cell based on ZnO nanowires. Appl. Surf. Sci. 256, 7438–7441.

Chen, J., Li, C., Zhao, D.W., Lei, W., Zhang, Y., Cole, M.T., Chu, D.P., Wang, B.P., Cui, Y.P., Sun, X.W., Milne, W.I., 2010b. A quantum dot sensitized solar cell based on vertically aligned carbon nanotube template ZnO arrays. Electrochem. Commun. doi:10.1016/j.elecom.2010.08.001.

Chiba, Y., Islam, A., Watanabe, Y., Komiya, R., Koide, N., Han, L., 2006. Dye-sensitized solar cells with conversion efficiency of 11.1%. Jpn. J. Appl. Phys. 45, 638–640.

Clifford, J., Johnston, K., Levina, L., Sargent, E., 2007. Schottky barriers to colloidal quantum dot films. Appl. Phys. Lett. 91, 253117.

Dayal, S., Reese, M.O., Ferguson, A.J., Ginley, D.S., Rumbles, G., Kopidakis, N., 2010a. The effect of nanoparticle shape on the photocarrier dynamics and photovoltaic device performance of ploy(3-hexylthiophene): CdSe nanoparticl bulk heterojunction solar cells. Adv. Funct. Mater. 20, 2629–2635.

Dayal, S., Kopidakis, N., Olson, D.C., Ginley, D.S., Rumbles, G., 2010b. Photovoltaic devices with a low band gap polymer and CdSe nanostructures exceeding 3% efficiency. Nano Lett. 10, 239–242.

De Girolamo, J., Reiss, P., Pron, A., 2007. Supramolecularly assembled hybrid materials via molecular recognition between diaminopyrimidine-functionalized poly(hexylthiophene) and thymine-capped CdSe nanocrystals. J. Phys. Chem. C 111, 14681–14688.

Debntah, R., Greiner, M.T., Kramer, J.J., Fuscher, A., Tang, J., Barkhouse, D.A.R., Wang, X., Levina, L., Lu, Z.-H., Sargent, E.H., 2010. Depleted-heterojunction colloidal quantum dot photovoltaics employing low-cost electrical contacts. Appl. Phys. Lett. 97, 023109.

Debnath, R., Tang, J., Barkhouse, D.A., Wang, X., Pattantyus-Abraham, A.G., Brzozowski, L., Levina, L., Sargent, E.H., 2010. Ambient-processed colloidal quantum dot solar cells via individual pre-encapsulation of nanoparticles. J. Am. Chem. Soc. 132, 5952–5953.

Deng, M., Zhang, Q., Huang, S., Li, D., Luo, Y., Shen, Q., Toyoda, T., Meng, Q., 2010. Low-cost flexible nano-sulfide/carbon composite counter electrode for quantum-dot-sensitized solar cell. Nanoscale Res. Lett. 5, 986–990.

Diguna, L.J., Shen, Q., Kobayashi, J., Toyoda, T., 2007. High efficiency of CdSe quantum-dot-sensitized TiO_2 inverse opal solar cells. Appl. Phys. Lett. 91, 023116.

Dibbell, R.S., Watson, D.F., 2009. Distance-dependent electron transfer in tethered assemblies of CdS quantum dots and TiO_2 nanoparticles. J. Phys. Chem. C 113, 3139–3149.

Emin, S.M., Sogoshi, N., Nakabayashi, S., Fujihara, T., Dushkin, C.D., 2009a. Kinetics of photochromic induced energy transfer between manganese-doped zinc–selenide quantum dots and spiropyrans. J. Phys. Chem. C 113, 3998–4007.

Emin, S., Sogoshi, N., Nakabayashi, S., Villeneuve, M., Dushkin, C., 2009b. Growth kinetics of CdS quantum dots and synthesis of their polymer nano-composites in CTAB reverse micelles. J. Photochem. Photobiol. A 207, 173–180.

Emin, S., Loukanov, A., Wakasa, M., Nakabayashi, S., Kaneko, Y., 2010. Photostability of water-dispersible CdTe quantum dots: capping ligands and oxygen. Chem. Lett. 39, 654–656.

Ernst, K., Belaidi, A., Könenkamp, R., 2003. Solar cell with extremely thin absorber on highly structured substrate. Semicond. Sci. Technol. 18, 475.

Fan, S.-Q., Fang, B., Kim, J.H., Kim, J.-J., Yu, J.-S., Ko, J., 2010. Hierarchical nanostructured spherical carbon with hollow core/mesoporous shell as a highly efficient counter electrode in CdSe quantum-dot-sensitized solar cells. Appl. Phys. Lett. 96, 063501.

Farrow, B., Kamat, P.V., 2009. CdSe quantum dot sensitized solar cells. Shuttling electrons through stacked carbon nanocups. J. Am. Soc. 131, 11124–11131.

Feng, Y., Yun, D., Zhang, X., Feng, W., 2010. Solution-processed bulk heterojunction photovoltaic devices based on poly(2-methoxy,5-octoxy)-1,4-phenylenevinylene-multiwalled carbon nanotubes/PbSe quantum dots. Appl. Phys. Lett. 96, 093301.

Gao, X.-F., Li, H.-B., Sun, W.-T., Chen, Q., Tang, F.-Q., Peng, L.-M., 2009. CdTe quantum dots-sensitized TiO_2 nanotube array photoelectrodes. J. Phys. Chem. C 113, 7531–7535.

Gao, X.-F., Sun, W.-T., Hu, Z.-D., Ai, G., Zhang, Y.-L., Feng, S., Li, F., Peng, L.-M., 2009. An efficient method to form heterojunction CdS/TiO_2 photoelectrodes using highly ordered TiO_2 nanotube array films. J. Phys. Chem. C 113, 20481–20485.

Greenham, N.C., Peng, X., Alivisatos, A.P., 1996. Charge separation and transport in conjugated-polymer/semiconductor-nanocrystal composites studied by photoluminescence quenching and photoconductivity. Phys. Rev. B 54, 17628–17637.

Greenham, N.C., Peng, X.G., Alivisatos, A.P., 1997. Charge separation and transport in conjugated polymer/cadmium selenide nanocrystal composites studied by photoluminescence quenching and photoconductivity. Synth. Metals 84, 545–546.

Giménez, S., Mora-Seró, I., Macor, L., Guijarro, N., Lana-Villarreal, T., Gómez, R., Diguna, L.J., Shen, Q., Toyoda, T., Bisquert, J., 2009. Improving the performance of colloidal quantum-dot-sensitized solar cells. Nanotechnology 20, 295204.

Günes, S., Fritz, K.P., Neugebauer, H., Sariciftci, N.S., Kumar, S., Scholes, G.D., 2007a. Hybrid solar cells using PbS nanoparticles. Sol. Energy Mater. Sol. Cells 91, 420–423.

Günes, S., Neugebauer, H., Sariciftci, N.S., 2007b. Conjugated polymer-based organic solar cells. Chem. Rev. 107, 1324–1338.

Grätzel, M., 2001. Photoelectrochemical cell. Nature 414, 338–344.

Han, L., Qin, D., Jiang, X., Liu, Y., Wang, L., Chen, J., Cao, Y., 2006. Synthesis of high quality zinc-blende CdSe nanocrystals and their application in hybrid solar cells. Nanotechnology 17, 4736–4742.

Hodes, G., 2008. Coparison of dye- and semiconductor-sensitized porous nanocrystalline liquid junction solar cells. J. Phys. Chem. C 112, 17778–17787.

Hoppe, H., Sariciftci, N.S., 2004. Organic solar cells: an overview. J. Mater. Res. 19, 1924–1945.

Hoyer, P., Könenkamp, R., 1995. Photoconduction in porous TiO_2 sensitized by PbS quantum dots. Appl. Phys. Lett. 66, 349–351.

Huang, W., Peng, J., Wang, L., Wang, J., Cao, Y., 2008. Impedance spectroscopy investigation of electron transport in solar cells based on blend film of polymer and nanocrystals. Appl. Phys. Lett. 92, 013308.

Hussain, A.M., Neppolian, B., Shim, H.-S., Kim, S.H., Kim, S.-K., Choi, H.C., Kim, W.B., Lee, K., Park, S.-J., 2010. Efficiency enhacement in bulk heterojunction polymer photovoltaic cells using $ZrTiO4/Bi_2O_3$ metal-oxide nanocomposites. Jpn. J. Appl. Phys. 49, 042301.

Huynh, W.U., Peng, X.G., Alivisatos, A.P., 1999. CdSe nanocrystals rods/poly(3-hexylthiophene) composite photovoltaic devices. Adv. Mater. 11, 923–926.

Huynh, W.U., Dittmer, J.J., Alivisatos, A.P., 2002. Hybrid nanorod-polymer solar cells. Science 295, 2425–2427.

Huynh, W.U., Dittmer, J.J., Teclemariam, N., Milliron, D.J., Alivisatos, A.P., Barnham, K.W.J., 2003. Charge transport in hybrid nanorod-polymer composite photovoltaic cells. Phys. Rev. B 67, 115326.

Hyun, B.-R., Zhong, Y.-W., Bartnik, A.C., Sun, L., Abruna, H.D., Wise, F.W., Goodreau, J.D., Matthews, J.R., Leslie, T.M., Borelli, N.F., 2008. Electron injection from colloidal PbS quantum dots into titanium dioxide nanoparticles. ACS Nano 2, 2206.

Itzhaik, Y., Niitsoo, O., Page, M., Hodes, G., 2009. Sb_2S_3-sensitized nanoporous TiO_2 solar cells. J. Phys. Chem C 113, 4254–4256.

Jiang, X., Schaller, R.S., Lee, S.B., Pietryga, J.M., Klimov, V.I., Zakhidov, A.A., 2007. PbSe nanocrystal/conducting polymer solar cells with an infrared response to 2 micron. J. Mater. Res. 22, 2204–2210.

Jiang, X., Chen, F., Qiu, W., Yan, Q., Nan, Y., Xu, H., Yang, L., Chen, H., 2010. Effects of molecular interface modification in CdS/polymer hybrid bulk heterojunction solar cells. Sol. Energy Mater. Sol. Cells. doi:10.1016/j.solmat.2010.07.016.

Johnston, K.W., Pattanthyus-Abraham, A.G., Clifford, J.P., Myrskog, S.H., MacNeil, D.D., Levina, L., Sargent, E.H., 2008. Schottky-quantum dot photovoltaics for efficient infrared power conversion. Appl. Phys. Lett. 92, 151115.

Ju, T., Graham, R.L., Zhai, G., Rodriguez, Y.W., Breeze, A.J., Yang, L., Alers, G.B., Carter, S.A., 2010. High efficiency mesoporous titanium oxide PbS quantum dot solar cells at low temperature. Appl. Phys. Lett. 97, 043106.

Kamat, P.V., 2007. Meeting the clean energy demand: nanostructure architectures for solar energy conversion. J. Phys. Chem. C 111, 2834–2860.

Kamat, P.V., 2008. Quantum dot solar cells. Semiconductor nanocrystals as light harvester. J. Phys. Chem. C 112, 18737–18753.

Kawazoe, H., Yasukawa, M., Hyodu, H., Kurita, M., Yanagi, H., Hosono, H., 1997. *P*-type electrical conduction in transparent thin films of $CuAlO_2$. Nature 389, 939–942.

Klem, E.J., MacNeil, D., Cyr, P., Levina, L., Sargent, E., 2007. Efficient solution-processed infrared photovoltaic cell: Planarized all-inorganic bulk heterojunction devices via inter-quantum-dot bridging during growth from solution. Appl. Phys. Lett. 90, 183113.

Klem, E.J., MacNeil, D.D., Levina, L., Sargent, E.H., 2008. Solution processed photovoltaic devices with 2% infrared monochromatic power conversion efficiency: performance optimization and oxide formation. Adv. Mater. 20, 3433–3439.

Kniprath, R., Rabe, J.P., McLeskey, J.T., Wang, D., Kirstein, S., 2009. Hybrid photovoltaic cells with II–VI quantum dot sensitizers fabricated by layer-by-layer deposition of water-soluble components. Thin Solid Films 518, 295–298.

Koleilat, G.I., Levina, L., Shukla, H., Myrskog, S.H., Hinds, S., Pattantyus-Abraham, A.G., Sargent, E.H., 2008. Efficient, stable infrared photovoltaics based on solution-cast colloidal quantum dots. ACS Nano 2, 833–840.

Kongkanand, A., Tvrdy, K., Takechi, K., Kuno, M., Kamat, P.V., 2008. Quantum dot solar cells. Tuning photoresponse through size and shape control of CdSe–TiO_2 architecture. J. Am. Chem. Soc. 130, 4007–4015.

Könenkamp, R., 2008. Inorganic-extended junction devices. Nanostructured and Photoelectrochemical Systems for Solar Photon Conversion. Imperial College Press, pp. 393–452 (Chapter 6).

Kumar, S., Scholes, G.D., 2008. Colloidal nanocrystal solar cells. Microchim. Acta 160, 315–325.

Lan, G.-Y., Yang, Z., Lin, Y.-W., Lin, Z.-H., Liao, H.-Y., Chang, H.-T., 2009. A single strategy for improving the energy conversion of multilayered CdTe quantum dot-sensitized solar cells. J. Mater. Chem. 19, 2349–2355.

Law, M., Beard, M.C., Choi, S., Luther, J.M., Hanna, M.C., Nozik, A.J., 2008. Determining the internal quantum efficiency of PbSe nanocrystal solar cells with the aid of an optical model. Nano Lett. 8, 3904–3910.

Lee, H.-J., Kim, D.-Y., Yook, J.-S., Bang, J., Kim, S., Park, S.-M., 2007. Anchoring cadmium chalcogenide quantum dots (QDs) onto stable oxide semiconductors for QD sensitized solar cells. Bull. Korean Chem. Soc. 28, 953–958.

Lee, Y.-L., Huang, B.-M., Chien, H.-T., 2008a. Highly efficient CdSe-sensitized TiO_2 photoelectrode for quantum-dot-sensitized solar cell applications. Chem. Mater. 20, 6903–6905.

Lee, W., Kang, S.H., Min, S.K., Sung, Y.-E., Han, S.-H., 2008b. Co-sensitization of vertically aligned TiO_2 nanotubes with two different sizes of CdSe quantum dots for broad spectrum. Electrochem. Commun. 10, 1579–1582.

Lee, H.J., Yum, J.-H., Leventis, H.C., Zakeeruddin, S.M., Haque, S.A., Chen, P., Seok II, S., Grätzel, M., Nazeeruddin, M.K., 2008c. CdSe quantum dot-sensitized solar cells exceeding efficiency 1% at full-sun intensity. J. Phys. Chem. C 112, 11600–11608.

Lee, W., Lee, J., Lee, S., Yi, W., Han, S.-H., Cho, B.W., 2008d. Enhanced charge collection and reduced recombination of CdS/TiO_2 quantum-dots sensitized solar cells in the presence of single-walled carbon nanotubes. Appl. Phys. Lett. 92, 153510.

Lee, H.J., Leventis, H.C., Moon, S.-J., Chen, P., Ito, S., Haque, S.A., Torres, T., Nüesch, F., Geiger, T., Zakeeruddin, S.M., Grätzel, M., Nazeeruddin, M.K., 2009a. PbS and CdS quantum dot-sensitized solid-state solar cells: "Old concepts, new results". Adv. Funct. Mater. 19, 2735–2742.

Lee, H.J., Wang, M., Chen, P., Gamelin, D.R., Zakeeruddin, S.M., Gratzel, M., Nazeeruddin, M.K., 2009b. Efficient CdSe quantum dot-sensitized solar cells prepared by an improved successive ionic layer adsorption and reaction processes. Nano Lett. 9, 4221–4227.

Lee, W., Lee, J., Min, S.K., Park, T., Yi, W., Han, S.-H., 2009c. Effect of single-walled carbon nanotubes in PbS/TiO2 quantum dots-sensitized solar cells. Mater. Sci. Eng. B 156, 48–51.

Lee, H.J., Chen, P., Moon, S.-J., Sauvage, F., Sivula, K., Bessho, T., Gamelin, D.R., Comte, P., Zakeeruddin, S.M., Seok, S.II., Gratzel, M., Nazeeruddin, M.K., 2009d. Regenerative PbS and CdS quantum dot sensitized solar cells with a cobalt complex as hole mediator. Langmuir 25, 7602–7608.

Lee, Y.-L., Lo, Y.-S., 2009e. Highly efficient quantum-dot-sensitized solar cell based on co-sensitization of CdS/CdSe. Adv. Funct. Mater. 19, 604–609.

Lee, Y.-L., Chi, C.-F., Liau, S.-Y., 2010. CdS/CdSe co-sensitized TiO_2 photoelectrodes for efficient hydrogen generation in a photoelectrochemical cell. Chem. Mater. 22, 922–927.

Leschkies, K.S., Divakar, R., Basu, J., Enache-Pommer, E., Boercker, J.E., Carter, C.B., Kortshagen, U.R., Norris, D.J., Aydil, E.S., 2007. Photosensitization of ZnO nanowires with CdSe quantum dots for photovoltaic devices. Nano Lett. 7, 1793–1798.

Leschkies, K.S., Beatty, T.J., Kang, M.S., Norris, D., Aydil, E.S., 2009. Solar cells based on junction between colloidal PbSe nanocrystals and thin ZnO films. ACS Nano 3, 3638.

Leventis, H.C., O'Mahony, F., Akhtar, J., Afzaal, M., O'Brien, P., Haque, S.A., 2010. Transient optical studies of interfacial charge transfer at nanostructured metal oxides/PbS quantum dot/organic hole conductor heterojunctions. J. Am. Chem. Soc. 132, 2743–2750.

Levy-Clément, C., Tena-Zaera, R., Ryan, M.A., Hodes, G., 2005. CdSe-sensitized p-CuSCN/nanowire n-ZnO heterojunctions. Adv. Mater. 17, 1512–1515.

Lin, Y.-Y., Chu, T.-H., Li, S.-S., Chuang, C.-H., Chang, C.-H., Su, W.-F., Chang, C.-P., Chu, M.-W., Chen, C.-W., 2009. Interfacial nanostructuring on the performance of polymer/TiO_2 nanorod bulk heterojunction solar cells. J. Am. Chem. Soc. 131, 3644–3649.

Lin, S.-C., Lee, Y.-L., Chang, C.-H., Shen, Y.-J., Yang, Y.-M., 2007. Quantum-dot-sensitized solar cells: Assembly of CdS-quantum-dots coupling techniques of self-assembled monolayer and chemical bath deposition. Appl. Phys. Lett. 90, 143517.

Liu, C.-Y., Holman, Z.C., Kortshagen, U.R., 2009. Hybrid solar cells from P3HT and silicon nanocrystals. Nano Lett. 9, 449–452.

Liu, L., Hensel, J., Fitzmorris, R.C., Li, Y., Zhang, J.Z., 2010a. Preparation and photoelectrochemical properties of CdSe/TiO_2 hybrid mesoporous structures. J. Phys. Chem. Lett. 1, 155–160.

Liu, C.-Y., Kortshagen, U.R., 2010b. A silicon nanocrystal Schottky junction solar cell produced from colloidal silicon nanocrystals. Nanoscale Res. 5, 1253–1256.

Lloyd, M.T., Lee, Y.-J., Davis, R.J., Fang, E., Fleming, R.M., Hsu, J.W.P., Kline, R.J., Toney, M.F., 2009. Improved efficiency in poly(3-hexylthiophene)/zinc oxide solar cells via lithium incorporation. J. Phys. Chem. C 113, 17608–17612.

Lokteva, I., Radychev, N., Witt, F., Borchert, H., Parisi, J., Kolny-Olesiak, J., 2010. Surface treatment of CdSe nanoparticles for application in hybrid solar cells: the effect of multiple ligand exchange with pyridine. J. Phys. Chem. C 114, 12784–12791.

Luther, J.M., Law, M., Beard, M.C., Song, Q., Reese, M.O., Ellingson, R.J., Nozik, A.J., 2008. Schottky solar cells based on colloidal nanocrystal films. Nano Lett. 8, 3488–3492.

Luther, J.M., Gao, J., Lloyd, M.T., Semonin, O.E., Beard, M.C., Nozik, A.J., 2010. Stability assessment on a 3% bilayer PbS/ZnO quantum dot heterojunction solar cell. Adv. Mater. 22, 3704–3707.

Ma, W., Luther, J.M., Zheng, H., Wu, Y., Alivisatos, A.P., 2009. Photovoltaic devices employing ternary PbS_xSe_{1-x} nanocrystals. Nano Lett. 9, 1699–1703.

Mann, J.R., Watson, D.F., 2007. Adsorption of CdSe nanoparticles to thiolated TiO_2 surfaces: influence of intralayer disulfide formation on CdSe surface coverage. Langmuir 23, 10924–10928.

Maria, A., Cyr, P.W., Klem, E.J.D., Levina, L., Sargeant, E., 2005. Solution-processed infrared photovoltaic devices with >10% monochromatic internal quantum efficiency. Appl. Phys. Lett. 87, 213112.

Mishra, A., Fischer, M.K.R., Bäuerle, P., 2009. Metal-free organic dyes for dye-sensitized solar cells: from structure: property relationships to design rules. Angew. Chem. Int. Ed. 48, 2474–2499.

Mora-Seró, I., Giménez, S., Moehl, T., Fabregat-Santiago, F., Lana-Villareal, T., Gómez, R., Bisquert, J., 2008. Factors determining the photovoltaic performance of a CdSe quantum dot sensitized solar cell: the role of the linker molecule and of the counter electrode. Nanotechnology 18, 424007.

Mozer, A.J., Wada, Y., Jiang, K.J., Masaki, N., Yanagida, S., Mori, S.N., 2006. Efficient dye-sensitized solar cells based on a 2-thiophen-2-yl-vinyl-conjugated ruthenium photosensitizer and conjugated polymer hole conductor. Appl. Phys. Lett. 89, 043509.

Murphy, J., Beard, M., Norman, A., Ahrenkiel, S., Johnson, J., Yu, P., Mićić, O., Ellingson, R., Nozik, A., 2006. PbTe colloidal nanocrystals: synthesis, characterization, and multiple exciton generation. J. Am. Chem. Soc. 128, 3241–3247.

Nadarajah, A., Word, R.C., VanSant, K., Könenkamp, R., 2008. Nanowire-quantum-dot-polymer solar cells. Phys. Stat. Sol. 245, 1834–1837.

Niitsoo, O., Sarkar, S.K., Pejoux, C., Rühle, S., Cahen, D., Hodes, G., 2006. Chemical bath deposited CdS/CdSe-sensitized porous TiO_2 solar cells. J. Photochem. Photobiol. A 181, 306–313.

Noone, K.M., Anderson, N.C., Horwitz, N.E., Munro, A.M., Kulkarni, A.P., Ginger, D.S., 2009. Absence of photoinduced charge transfer in blends of PbSe quantum dots and conjugated polymers. ACS Nano 3, 1345–1352.

Noone, K.M., Strein, E., Anderson, N.C., Wu, P.-T., Jenekhe, S.A., Ginger, D.S., 2010. Broadband absorbing bulk heterojunction photovoltaics using low-bandgap solution-processed quantum dots. Nano Lett. 10, 2635–2639.

Okazaki, K., Kojima, N., Tachibana, Y., Kuwabata, S., Torimoto, T., 2007. One-step preparation and photosensitivity of size-quantized cadmium chalcogenide nanoparticles deposited on porous zinc oxide film electrodes. Chem. Lett. 36, 712–713.

Olson, J.D., Gray, G.P., Carter, S.A., 2009. Optimizing hybrid photovoltaics through annealing and ligand choice. Sol. Energy Sol. Cells 93, 519–523.

Olson, J.D., Rodriguez, Y.W., Yang, L.D., Alers, G.B., Carter, S.A., 2010. CdTe Schottky diodes from colloidal nanocrystals. Appl. Phys. Lett. 96, 242103.

Palaniappan, K., Murphy, J.W., Khanam, N., Horvath, J., Alshareef, H., Quevedo-Lopez, M., Biewer, M.C., Park, S.Y., Kim, M.J., Gnade, B.E., Stefan, M.C., 2009. Poly(3-hexylthiophene)−CdSe quantum dot bulk heterojunction solar cells: influence of the functional end-group of the polymer. Macromolecules 42, 3845–3848.

Park, S.H., Roy, A., Beaupré, S., Cho, S., Coates, N., Moon, J.S., Moses, D., Leclerc, M., Lee, K., Heeger, A.J., 2009. Bulk heterojunction solar cells with internal quantum efficiency approaching 100%. Nat. Photon. 3, 297–303.

Pathan, H.M., Lokhande, C.D., 2004. Deposition of metal chalcogenide thin films by successive ionic layer adsorption and reaction (SILAR) method. Bull. Mater. Sci. 27, 85–111.

Pattantyus-Abraham, A.G., Kramer, I.J., Barkhouse, A.R., Wang, X., Konstantatos, G., Debnath, R., Levina, L., Raabe, I., Nazeeruddin, M.K., Grätzel, M., Sargent, E.H., 2010. Depleted-heterojunction colloidal quantum dot solar cells. ACS Nano 4, 3374–3380.

Peng, X., Manna, L., Yang, W., Wickham, J., Scher, E., Kadavanich, E.J., Alivisatos, A.P., 2000. Shape control of CdSe nanocrystals. Nature 404, 59–61.

Peter, L.L.M., Riley, D.J., Tull, E.J., Wijayantha, K.G.U., 2002. Photosensitization of nanocrystalline TiO_2 by self-assembled layers of CdS quantum dots. Chem. Commun., 1030–1031.

Pijpers, J.J.H., Ulbricht, R., Tielrooij, K.J., Osherov, A., Golan, Y., Delerue, C., Allan, G., Bonn, M., 2009. Assessment of carrier-multiplication efficiency in bulk PbSe and PbS. Nat. Phys. 5, 811–814.

Plass, R., Serge, P., Krüger, J., Grätzel, M., 2002. Quantum dot sensitization of organic−inorganic hybrid solar cells. J. Phys. Chem. B 106, 7578–7580.

Prabakar, K., Minkyu, S., Inyoung, S., Heeje, K., 2010. CdSe quantum dots co-sensitized TiO_2 photoelectrodes: particle size dependent properties. J. Phys. D: Appl. Phys. 43, 012002.

Robel, I., Subramanian, V., Kuno, M., Kamat, P., 2006. Quantum dot solar cells. Harvesting light energy with CdSe nanocrystals molecularly linked to mesoscopic TiO_2 films. J. Am. Chem. Soc. 128, 2385–2393.

Robel, I., Kuno, M., Kamat, P.V., 2007. Size-dependent electron injection from excited CdSe quantum dots into TiO_2 nanoparticles. J. Am. Chem. Soc. 129, 4136–4137.

Rühle, S., Shalom, M., Zaban, A., 2010. Quantum-dot-sensitized solar cells. Chem. Phys. Chem. 11, 2290–2304.

Sambur, J.B., Parkinson, B.A., 2010a. CdSe/ZnS core/shell quantum dot sensitization of low index TiO_2 single crystal surfaces. J. Am. Chem. Soc. 132, 2130–2131.

Sambur, J.B., Riha, S.C., Choi, D., Parkinson, B.A., 2010b. Influence of surface chemistry on the binding and electronic coupling of CdSe quantum dots to single crystal TiO_2 surfaces. Langmuir 26, 4839–4847.

Sapp, S.A., Elliott, C.M., Contado, C., Caramori, S., Bignozzi, C.A., 2002. Substituted polypyridine complexes of cobalt (II/III) as efficient electron-transfer mediators in dye-sensitized solar cells. J. Am. Chem. Soc. 124, 11215–11222.

Schaller, R.D., Klimov, V.I., 2004. High efficiency carrier multiplication in PbSe nanocrystals: Implications for solar energy conversion. Phys. Rev. Lett. 92, 186601.

Schaller, R., Sykora, M., Jeong, S., Klimov, V., 2006. High-efficiency carrier multiplication and ultrafast charge separation in semiconductor nanocrystals studied via time-resolved photoluminescence. J. Phys. Chem. B 110, 25332–25338.

Šimurda, M.S., Němec, P., Formanánek, P., Němcová, I., Malý, P., 2006. Morphology of CdSe films prepared by chemical bath deposition: The role of substrate. Thin Solid Films, 71–75.

Seo, J., Kim, S.J., Kim, W.J., Singh, R., Samoc, M., Cartwright, A.N., Prasad, P.N., 2009. Enhacement of the photovoltaic performance in PbS nanocrystal:P3HT hybrid composite device by post-treatment-driven ligand exchange. Nanotechnology 20, 095202.

Service, R.F., 1996. New solar cells seem to have power at the right price. Science 272, 1744–1745.

Shalom, M., Dor, S., Rühle, S., Grinis, L., Zaban, A., 2009. Core/CdS quantum dot/shell mesoporous solar cells with improved stability and efficiency using an amorphous TiO2 coating. J. Phys. Chem. C 113, 3895–3898.

Shen, Y.-J., Lee, Y.-L., 2008. Assembly of CdS quantum dots onto mesoscopic TiO_2 films for quantum dot-sensitized solar cell applications. Nanotechnology 19, 045602.

Shen, Q., Yamada, A., Tamura, S., Toyoda, T., 2010. CdSe quantum dot-sensitized solar cell employing TiO_2 nanotube working-electrode and Cu_2S counter-electrode. Appl. Phys. Lett. 97, 123107.

Shiga, T., Takechi, K., Motohiro, T., 2006. Photovoltaic performance and stability of CdTe/polymeric hybrid solar cells using a C_{60} buffer layer. Sol. Energy Mater. Sol. Cells 90, 1849–1858.

Shockley, W., Queisser, H.J., 1961. Detailed balance limit of efficiency of *p–n* junction solar cells. J. Appl. Phys. 32, 510–519.

Sudhagar, P., Jung, J.H., Park, S., Lee, Y.-G., Sathyamoorthy, R., Kang, Y.S., Ahn, H., 2009. The performance of coupled (CdS:CdSe) quantum dot-sensitized TiO_2 nanofibrous solar cells. Electrochem. Commun. 11, 2220–2224.

Sukhovatkin, S., Hinds, S., Brzozowski, L., Sargent, E.H., 2009. Colloidal quantum-dot photodetectors exploiting multiexciton generation. Science 324, 1542–1544.

Sun, B., Marx, E., Greenham, N.C., 2003. Photovoltaic devices using blends of branched CdSe nanoparticles and conjugated polymers. Nano Lett. 3, 961–963.

Sun, S.-S., Sariciftci, N.S., 2005. Organic Photovoltaics: Mechanisms, Materials and Devices. Taylor and Francis, Roca Raton.

Sun, B., Greenham, N., 2006. Improved efficiency of photovoltaics based on CdSe nanorods and poly(3-hexylthiophene) nanofibres. Phys. Chem. Chem. Phys. 8, 3557–3560.

Sun, W.-T., Yu, Y., Pan, H.-Y., Gao, X.-F., Chen, Q., Peng, L.-M., 2008. CdS quantum dots sensitized TiO_2 nanotube-array photoelectrodes. J. Am. Chem. Soc. 130, 1124–1125.

Tachibana, Y., Akiyama, H.Y., Ohtsuka, Y., Torimoto, T., Kuwabata, S., 2007. CdS quantum dots sensitized TiO_2 sandwich type photoelectrochemical solar cells. Chem. Lett. 36, 88–90.

Tachibana, Y., Umekita, K., Otsuka, Y., Kuwabata, S., 2008. Performance improvement of CdS quantum dots sensitized TiO_2 solar cells by introducing a dense TiO_2 blocking layer. J. Phys. D: Appl. Phys. 41, 102002.

Talapin, D.V., Lee, J.-S., Kovalenko, M.V., Shevchenko, E.V., 2010. Prospects of colloidal nanocrystals for electronic and optoelectronic applications. Chem. Rev. 110, 389–458.

Tan, Z., Zhu, T., Thein, M., Gao, S., Cheng, A., Zhang, F., Zhang, C., Su, H., Wang, J., Henderson, R., Hahm, J., Yang, Y., Xu, J., 2009. Integration of planar and bulk heterojunctions in polymer/nanocrystal hybrid photovoltaic cells. Appl. Phys. Lett. 95, 063510.

Tang, J., Wang, X., Brzozowski, L., Aaron, D., Barkhouse, R., Debnath, R., Levina, L., Sargent, E.H., 2010. Schottky quantum dot solar cells stable in air under solar illumination. Adv. Mater. 22, 1398–1402.

Taretto, K., Rau, U., 2005. Influence of built-in voltage in optimized extremely thin absorber solar cells. Thin Solid Films, 447–451.

Thompson, B.C., Fréchet, J.M.J., 2008. Polymer-fullerene composite solar cells. Angew. Chem. Int. Ed. 47, 58–77.

Tomkiewicz, M., 1979. The potential distribution at the TiO_2 aqueous electrolyte interface. J. Electrochem. Soc. 126, 1505–1510.

Toyoda, T., Uehata, T., Suganuma, R., Tamura, S., Sato, A., Yamamoto, K., Kobayashi, N., Shen, Q., 2007. Crystal growth of CdSe quantum dots adsorbed on nanoparticle, inverse opal, and nanotube TiO_2 photoelectrodes characterized by photoacoustic spectroscopy. Jpn. J. Appl. Phys. 46, 4616–4621.

Toyoda, T., Kobayashi, J., Shen, Q., 2008. Correlation between crystal growth and photosensitization of nanostructured TiO_2 electrodes using supporting Ti substrates by self-assembled CdSe quantum dots. Thin Solid Films 516, 2426–2431.

Truong, N.T.N., Kim, W.K., Park, C., 2010. Effect of CdSe/P3HT composition on electrical and structural properties of bulk heterojunction solar cell active layer. Sol. Energy Mater. Sol. Cells.

Tvrdy, K., Kamat, P.V., 2009. Substrate driven photochemistry of CdSe quantum dot films: charge injection and irreversible transformations on oxide surfaces. J. Phys. Chem. A 113, 3765–3772.

Versavel, M.Y., Haber, J.A., 2007. Structural and optical properties of amorphous and crystalline antimony sulfide thin-films. Thin Solid Films 515, 7171–7176.

Vogel, R., Pohl, K., Weller, H., 1990. Sensitization of highly porous, polycrystalline TiO_2 electrodes by quantum sized CdS. Chem. Phys. Lett. 174, 241–245.

Vomeyer, T., Katsikas, L., Giersig, M., Popovic, I.G., Diesner, K., Chemseddine, A., Eychmüller, A., Weller, H., 1994. CdS Nanoclusters: Synthesis, characterization, size dependent oscillator strength, temperature shift of the excitonic transition energy, and reversible absorbance shift. J. Phys. Chem. 98, 7665.

Wang, P., Abrusci, A., Wong, H.M.P., Svensson, M., Anderson, M.R., Greenham, N.C., 2006. Photoinduced charge transfer and efficient solar energy conversion in a blend of a red polyfluorene copolymer with CdSe nanoparticles. Nano Lett. 6, 1789–1793.

Wang, Z., Qu, S., Zeng, X., Zhang, C., Shi, M., Tan, F., Wang, Z., Liu, J., Hou, Y., Teng, F., Feng, Z., 2008. Synthesis of MDMO-PPV capped PbS quantum dots and their application to solar cells. Polymer 49, 4647–4651.

Wang, T.-L., Yang, C.-H., Shieh, Y.-T., Yeh, A.-C., Juan, L.-W., Zeng, H.C., 2010a. Synthesis of new nanocrystal-polymer nanocomposite as the electron acceptor in polymer bulk heterojunction solar cells. Eur. Polym. J. 46, 634–642.

Wang, X., Zhu, H., Xu, Y., Wang, H., Tao, Y., Hark, S., Xiao, X., Li, Q., 2010b. Aligned ZnO/CdTe core-shell nanocable arrays on indium tin oxide: Synthesis and photoelectrochemical properties. ACS Nano 6, 3302–3308.

Wang, G., Yang, X., Qian, F., Zhang, J., Li, Y., 2010c. Double-sided CdS and CdSe quantum dot co-sensitized ZnO nanowire arrays for photoelectrochemical hydrogen generation. Nano Lett. 10, 1088–1092.

Wienke, J., Krunks, M., Lenzmann, F., 2003. $In_x(OH)_yS_z$ as recombination barrier in TiO_2/inorganic absorber heterojunctions. Semicond. Sci. Technol. 18, 876–880.

Xin, Y., Huang, Z., Jiang, Z., Li, D., Peng, L., Zhai, J., Wang, D., 2010. Photoresponse of a single poly(p-phenylene vinylene)-CdSe bulk-heterojunction submicron fiber. Chem. Commun. 46, 2316–2318.

Yang, Z., Chang, H.-T., 2010. CdHgTe and CdTe quantum dot solar cells displaying an energy conversion efficiency exceeding 2%. Sol. Energy Mater. Sol. Cells. doi:10.1016/j.solmat.2010.06.013.

Yu, W.W., Qu, L., Guo, W., Peng, X., 2003. Experimental determination of the extinction coefficient of CdTe, CdSe, and CdS nanocrystals. Chem. Mater. 15, 2854–2860.

Yum, J.-H., Choi, S.-H., Kim, S.-S., Kim, D.-Y., Sun, Y.-E., 2007. CdSe quantum dots sensitized TiO_2 electrodes for photovoltaic cells. J. Korean Electrochem. Soc. 10, 257–261.

Yun, D., Feng, W., Wu, H., Yoshino, K., 2009. Efficient conjugated polymer-ZnSe and -PbSe nanocrystals hybrid photovoltaic cells through full solar spectrum utilization. Sol. Energy. Mater. Sol. Cells 93, 1208–1213.

Zaban, A., Mícíc, O.I., Gregg, B.A., Nozik, A.J., 1998. Photosensitization of nanoporous TiO_2 electrodes with InP quantum dots. Langmuir 14, 3153–3156.

Zhang, Q., Zhang, Y., Huang, S., Huang, X., Luo, Y., Meng, Q., Li, D., 2010. Application of carbon counterelectrode on CdS quantum dot-sensitized solar cells (QDSSCs). Electrochem. Commun. 12, 327–330.

Zhou, Y., Riehle, F.S., Yuan, Y., Schleiermacher, H.-F., Niggemann, M., Urban, G.A., Krüger, M., 2010. Improved efficiency of hybrid solar cells based on non-ligand-exchanged CdSe quantum dots and poly(3-hexylthiophene). Appl. Phys. Lett. 96, 013304.

Zhu, G., Su, F., Lv, T., Pan, L., Sun, Z., 2010. Au nanoparticles as interfacial layer for CdS quantum dot-sensitized solar cells. Nanoscale Res. Lett. 52. doi: 10.1007/s11671-010-9705-z.